Science of Advanced Materials
Vol. 2, 117–137, 2010

Spectral and Nonlinear Optical Characteristics of ZnO Nanocomposites

Litty Irimpan[1, 2, *], V. P. N. Nampoori[2], and P. Radhakrishnan[2]

[1] *St. Mary's College, Thrissur 680020, Kerala, India*
[2] *International School of Photonics, Cochin University of Science and Technology, Cochin 682022, Kerala, India*

REVIEW

The spectral and nonlinear optical properties of ZnO based nanocomposites prepared by colloidal chemical synthesis are investigated. Very strong UV emissions are observed from ZnO–Ag, ZnO–Cu and ZnO–SiO_2 nanocomposites. The strongest visible emission of a typical ZnO–Cu nanocomposite is over ten times stronger than that of pure Cu due to transition from deep donor level to the copper induced level. The optical band gap of ZnO–CdS and ZnO–TiO_2 nanocomposites is tunable and emission peaks changes almost in proportion to changes in band gap. Nonlinear optical response of these nanocomposites is studied using nanosecond laser pulses from a tunable laser in the wavelength range of 450–650 nm at resonance and off-resonance wavelengths. The nonlinear response is wavelength dependent and switching from RSA to SA has been observed at resonant wavelengths. Such a change-over is related to the interplay of plasmon/exciton band bleach and optical limiting mechanisms. The observed nonlinear absorption is explained through two photon absorption followed by weak free carrier absoption, interband absorption and nonlinear scattering mechanisms. The nonlinearity of the silica colloid is low and its nonlinear response can be improved by making composites with ZnO and ZnO–TiO_2. The increase of the third-order nonlinearity in the composites can be attributed to the enhancement of exciton oscillator strength. This study is important in identifying the spectral range and the composition over which the nonlinear material acts as an RSA based optical limiter. These nanocomposites can be used as optical limiters and are potential materials for the light emission and for the development of nonlinear optical devices with a relatively small limiting threshold.

Keywords: Nanocomposites, Fluorescence Emission, Nonlinear Absorption Coefficient, Two Photon Absorption and Nonlinear Refractive Index.

CONTENTS

1. INTRODUCTION

The field of nanocomposite materials has been widely recognized as one of the most promising and rapidly emerging research areas.[1–2] There are some material designs to strengthen and toughen ceramics by using composite techniques to incorporate particulate, whisker or platelet reinforcement. Recent investigations have shown that ceramic composites having nano-sized metal particulate dispersions show excellent optical, electrical and mechanical properties.[3] Promising applications are expected or have already been realized in many fields of technology such as optical and electronic materials, solid electrolytes, coating technology and catalysis. Significant investigations have been done in the photophysical and photochemical behavior of single and multicomponent metal and semiconductor nanoclusters.[1] Such composite materials are especially of interest in developing efficient light-energy conversion systems and optical devices. For example, photoinduced deposition of noble metals such as Pt or Au on semiconductor nanoclusters has often been employed to enhance their photocatalytic activity.[2]

With many advantages such as low cost, nontoxicity and stability, ZnO is becoming a very promising *n*-type

*Author to whom correspondence should be addressed.

oxide semiconductor. Most of the work has been devoted to the electrical and fluorescent properties of ion-doped zinc oxide materials,[4] while only a few reports can be found using ZnO as the matrix for nanoparticle composite films.[5] These nanocomposites may lead to optically functional properties. In this study, therefore, the nanocomposite techniques are applied to improve the spectral and optical properties of ZnO.[6–9]

Optical nonlinearity of metal nanoparticles in a semiconductor has attracted much attention because of the high polarisability and fast nonlinear response that can be utilised in making them as potential optical devices.[1,10] It is well known that noble metal nanoparticles show an absorption due to surface plasmon resonance (SPR) in the visible region.[1] Out of various metal nanoparticles, silver, copper and gold are extensively studied in colloids, thin films and in different glass matrices for their nonlinear optical properties.[11]

In recent years, interest in the synthesis, characterization, and application of colloidal "quantum dot" semiconductor materials has grown markedly.[12] Nanocrystals of cadmium sulfide are by far the most studied system among all the semiconducting nanocrystals.[13] The bulk CdS has a direct band gap of 2.4 eV at 300 K, and the typical Bohr exciton diameter of CdS is around 5.8 nm; consequently, CdS nanocrystals in the size range of 1–6 nm show sizable quantum confinement effects with remarkably different optical properties. The size dependent, unusual optical and electronic properties of these nanocrystals have been studied in detail using a wide variety of experimental and theoretical techniques.[14] Nanoscale composite materials containing titanium oxides are interesting because of their potential applications in optoelectronic devices and the bulk TiO_2 has a direct band gap of 3.2 eV.[15] A great deal of research effort has been focused on both synthesis of TiO_2 nanocomposites, and on their linear optical properties. Recently the nonlinear optical properties of such materials have also received attention. A large, reverse saturable type of nonlinear absorption is observed in polystyrene maleic anhydride-TiO_2 nanocomposites with a continuous wave He–Ne laser beam.[16]

Litty Irimpan received Ph.D. degree in Nanophotonics from Cochin University of Science and Technology, Kerala, India in 2009. Presently she is lecturer in Physics at St. Mary's College, Thrissur. She has 18 international journal publications and her research interests include Nanophotonics, Laser Physics, Spectroscopy, Nonlinear Optics, Nanomaterials and Photonic Materials. She is the life member of Indian Laser Association, Photonics Society of India and Plasma Science Society of India.

V. P. N. Nampoori is the Professor and Director of International School of Photonics, Cochin University of Science and Technology, Kerala, India. Dr. Nampoori has published more than 300 research papers and guided about 15 Ph.D.'s in lasers, laser spectroscopy and fibre optics. Significant contributions of Dr. Nampoori are in the area of Fibre optic Sensors, Molecular Spectroscopy, Nonlinear Optics and Photonic materials. Dr. Nampoori is one of the members of the core team to establish a well developed Laser and Photonics Laboratory in CUSAT and designed the course structure for Integrated M.Sc. Photonics Course as a part of the Centre of Excellence in Lasers and Optoelectronic Sciences. Dr. Nampoori is also interested in the field of Science Education through e-learning platform, popularization of science by writing popular articles in Malayalam and English periodicals.

P. Radhakrishnan received Ph.D. degree from Cochin University of Science and Technology in 1986. He has been a lecturer at the Cochin College from 1979 to 1988. Presently he is a Professor and at the International School of Photonics, and Director of Centre of Excellence in Lasers and Optoelectronic Sciences, Cochin University of Science and Technology. His research interests include laser technology, laser spectroscopy, and fiber optic sensors. He is the present President of the Photonics Society of India and life member of Indian Laser Association, Indian Association of Physics Teachers and the Indian Physics Association.

Extensive investigations of the photoluminescence and the third order optical nonlinearities of nanometer-sized semiconductor materials have demonstrated interesting physical properties and potential applications. The absorption and luminescent properties of TiO_2, CdS and PbS particles can be easily tuned by selecting appropriate matrix materials.[17] Recently, a microemulsion technique has been developed to prepare semiconductor nanocomposites such as ZnS/CdSe, ZnSe/CdSe, ZnS/CdS or TiO_2–SiO_2 in a core–shell structure.[18] Chemically synthesized semiconductor nanocomposites offer necessary and basic materials promising colour-tunable, flexible, all-purpose chromophore systems, in which the strong quantum confinement effect of the carriers leads to unique, size dependent linear and nonlinear optical properties.[19]

The synthesis of new nonlinear optical materials based on transparent semiconductor and insulator that contain metal nanoparticles is nowadays of great interest for applications in nonlinear optics.[1] For optical limiting applications it is necessary that the sample possess low linear losses and high nonlinear losses. Nonlinear losses can be due to multiphoton absorption, reverse saturable absorption, nonlinear scattering, and self-action of laser radiation (Kerr and thermal self-focusing and self-defocusing).[20]

Soon after the reporting of stimulated UV emission of ZnO at room temperature, ZnO attracted the people's attention as an UV laser material.[2] Effective UV random lasing has been observed from patterned *p*-SiC(4H)/*i*-ZnO–SiO_2 nanocomposite films under optical excitation.[21] UV random lasing can be achieved in these composites because the appropriate patterning of ZnO clusters enhances the optical quality (i.e., higher gain and lower loss) of the random media. However, the improvement of UV emission and the simplification of growth techniques are still very important. Different metal particles, organic nanocrystals and fullerenes doped in sol–gel glasses and silica composites are well studied for optical limiting applications.[1,3] It is also known that doping significantly improves the limiting performance of ZnO.

In this paper, we present the spectral and nonlinear optical properties of ZnO–Ag, ZnO–Cu, ZnO–CdS, ZnO–TiO_2, ZnO–SiO_2 and ZnO–TiO_2–SiO_2 nanocomposites. Ag and Cu are selected to prepare metal-semiconductor nanocomposites with ZnO, because of their interesting optical properties in the visible range which gives rise to wide applications in optoelectronic devices. Our results show that ZnO–CdS and ZnO–TiO_2 nanocomposites possess bandgap engineering, fluorescence tuning, very large optical nonlinearity and have a great potential for optical switching and optical communications. The nonlinearity of the silica colloid is low and its optical limiting response can be improved by making composites with ZnO and ZnO–TiO_2 which gives rise to wide applications in optoelectronic devices.

1.1. Theory

A crucial step in designing modern optoelectronic devices is the realization of bandgap engineering to create barrier layers and quantum wells in device heterostructures.[22] In order to realize such optoelectronic devices, modulation of the bandgap is required. To boost the concentration of electrons and holes, impurity atoms are introduced into the semiconductor crystal.[23] The energy gap of the semiconductor $A_xZn_{1-x}O$ (where A = Mg, Cd) is determined by the following equation,[24]

$$E_g(x) = (1-x)E_{ZnO} + xE_{AO} - bx(1-x) \qquad (1)$$

where b is the bowing parameter and E_{ZnO} and E_{AO} are the bandgap energies of compounds AO and ZnO respectively. The bowing parameter depends on the difference in electronegativities of the end binaries ZnO and AO.

High carrier concentrations in conduction and valence bands lead to bandgap reduction due to enhanced carrier–carrier interaction.[25] The reduction in bandgap, ΔE_g can be derived from many-body theory[26] as a function of the static dielectric constant ε_{st}, rest mass of electron m_0, the effective masses m_c and m_v, the number density N ($N = n = p$) and the temperature T. It is given by

$$\Delta E_g = -C\left[\frac{\varepsilon_{st}^5}{N}\left(m_0\frac{m_c+m_v}{m_c m_v} + BT^2\frac{\varepsilon_{st}}{N}\right)\right]^{-1/4} \qquad (2)$$

where the fit parameters C and B are 3.9×10^{-5} eVcm$^{3/4}$ and $B = 3.1 \times 10^{12}$ cm^{-3}K^{-2} respectively.

Heavy doping also leads to bandgap narrowing caused by carrier–carrier interaction as well as by distortion of the crystal lattice.[27] For Si, the bandgap reduction as a function of doping density N_{dop} is given by[28]

$$\Delta E_g(\text{meV}) = -6.92\left[\ln\left(\frac{N_{dop}}{0.13}\right) + \sqrt{\left(\ln\left(\frac{N_{dop}}{0.13}\right)\right)^2 + 0.5}\right] \qquad (3)$$

Both bandgap reduction mechanisms add up and they are often hard to separate.

2. EXPERIMENTAL DETAILS

In the present investigation, colloids of ZnO are synthesized by a modified polyol precipitation method.[29] The silver nano colloids are prepared by the reduction of a silver nitrate in H_2O with 1% sodium citrate near boiling temperature.[30] The copper nanocolloids are prepared by the hydrolysis of copper sulphate in water near boiling temperature.[31] The CdS nanocolloids are prepared by chemical method using $Cd(NO_3)_2 4H_2O$ and NH_2CSNH_2 (Merck, India) dissolved in 2-propanol and distilled water respectively.[32] The TiO_2 nanocolloids are prepared by

the hydrolysis Titanium tetrabutoxide (Aldrich) in distilled water.[33] A stable nanocolloid of SiO_2 particles dispersed in water has been obtained from Aldrich Chemical Company.[34] The molar concentration of all the precursor solutions are 0.025 M.

The ZnO-*A* nanocomposites are prepared via colloidal chemical synthesis by mixing certain amounts of colloids of *A* to ZnO at 120 °C during its preparation stage and stirred for 1 hour at that temperature.[30–33] The volume fraction of *A* is changed keeping the volume of ZnO constant. The samples having the ZnO-*xA* composition of (x=) 0.1–5% are named as ZnO-0.1*A* to ZnO-5*A* respectively. The nonlinearity of silica colloid is too low and hence the volume fraction of ZnO is changed to increase the nonlinearity in SiO_2 based nanocomposites keeping the volume of SiO_2 a constant.[35]

The ZnO nanocomposites are characterized by optical absorption measurements recorded using a spectrophotometer (JascoV-570 UV/VIS/IR) and fluorescence measurements recorded using a Cary Eclipse fluorescence spectrometer (Varian). In the present investigation, we have employed the single beam z-scan technique with nanosecond laser pulses to measure nonlinear optical absorption of ZnO nanocomposites.[36–37] A Q-switched Nd:YAG laser (Spectra Physics LAB-1760, 532 nm, 7 ns, 10 Hz) is used as the light source. The sample is moved in the direction of light incidence near the focal spot of the lens with a focal length of 200 mm. The radius of the beam waist ω_0 is calculated to be 35.4 μm. The Rayleigh length, $z_0 = \pi w_0^2/\lambda$ is estimated to be 7.4 mm, much greater than the thickness of the sample cuvette (1 mm), which is an essential prerequisite for z scan experiments. The transmitted beam energy, reference beam energy and their ratio are measured simultaneously by an energy ratiometer (Rj7620, Laser Probe Corp.) having two identical pyroelectric detector heads (Rjp735). The effect of fluctuations of laser power is eliminated by dividing the transmitted power by the power obtained at the reference detector. The data are analyzed by using the procedure described by Sheik Bahae et al. and the nonlinear coefficients are obtained by fitting the experimental z scan plot with the theoretical plots.[36]

3. RESULTS AND DISCUSSION

3.1. ZnO–Ag

3.1.1. Absorption Spectroscopy

Optical absorption measurement is an initial step to observe the single colloid and metal-semiconductor nanocomposite behaviour.[38] Figure 1 gives the room temperature absorption spectra of the ZnO–Ag nanocomposites. The excitonic peak of ZnO colloid is found to be blue shifted with respect to that of bulk ZnO which could be attributed to the confinement effects.[39] For silver nanocolloid, the surface plasmon absorption (SPA) band lies in the 410 nm region. Although the conduction and valence bands of semiconductors are separated by a well-defined band gap, metal nanoclusters have close-lying bands and electrons move quite freely. The free electrons give rise to a surface plasmon absorption band in metal clusters, which depends on both the cluster size and chemical surroundings.[1] The plasmon band of metal particles as explained on the basis of Mie theory involves dipolar oscillations of the free electrons in the conduction band that occupy energy states near the Fermi level.[1]

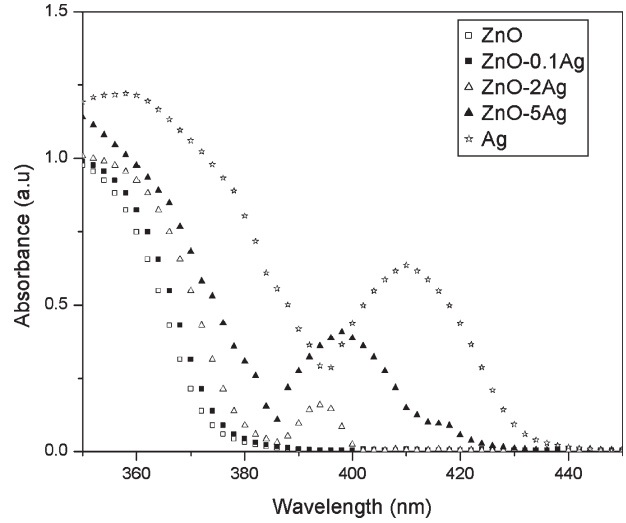

Fig. 1. Absorption spectra of ZnO–Ag nanocomposites.

The pronounced dependence of the absorption band gap on the size of the semiconductor nano crystals and SPA band on the size of metal nano crystals is used to determine the particle size. An order of magnitude estimate of the particle size is possible from the absorption spectra. The size of ZnO and Ag nanocolloids are in the range of 10–20 nm. The presence of excitonic peak and SPA band itself indicates that the composites are of nanometer size. The size evolution of nanocomposites may also have some relation with optical characteristics in addition to the composition and is a possible direction for future studies.

For small volume fraction of Ag, the composite exhibits the characteristics of ZnO with a red shift in the excitonic peak. On the other hand, the ZnO–2Ag nanocomposite exhibits both the semiconductor and metallic behaviour with a blue shift in plasmon band. Optical absorption spectra indicate presence of a well-defined ZnO excitonic feature along with the Ag surface plasmon absorption feature at 400 nm.[40] The optical absorption spectra of the clusters show a gradual shift in absorbance towards the visible region, over which an extremely weak surface plasmon resonance is superposed.

The surface plasmon absorption band of metal nanoclusters is very sensitive to the surface-adsorbed species and

dielectric of the medium. For example, I^- and $C_6H_5S^-$ ions result in damping of the surface plasmon band of colloidal silver particles.[41] Alternately, one can also observe bleaching of the surface plasmon band with electrons deposited from radiolytically produced radicals, which cause a blue shift and narrowing of the plasmon band. A more detailed discussion on the damping effects caused by surrounding material can be found elsewhere.[1] When the volume fraction of Ag increases beyond 2%, the surface plasmon peak is shifted towards 410 nm. It has been established that the shift of the SPA band of silver observed is a result of the accumulation of excess electrons on the ZnO/Ag particles which leads to equalization of the potentials of the conduction zones of the semiconductor and the metallic components of the nanocomposite.[42]

3.1.2. Fluorescence Spectroscopy

Photoluminescence spectra of all samples measured at room temperature are shown in Figure 2. The intensities of the emission peaks depend on the volume fraction of Ag of the samples. ZnO and ZnO–0.1Ag have only 385 nm emission, but the intensity of the peak of ZnO–0.1Ag is much stronger than that of ZnO. ZnO–1Ag has the strongest UV emission centered at 375 nm. ZnO–2Ag has UV emission centered at 365 nm, which can be fitted to two peaks centered at 348 and 382 nm. ZnO–5Ag and Ag have only a peak at 348 nm.

Figure 3 shows the PL intensity as a function of the silver content. It is clear that the intensity of this peak increases with the increasing amount of the Ag and Zn acceptors. When the ZnO colloid is overdoped by Ag, the Ag_2O nanoclusters appears and hence there is reduction in PL intensity.[43] The emission of ZnO at 385 nm can be attributed to exciton transition. An undoped ZnO colloid has insufficient holes and so restricted exciton concentration. After Ag doping, Ag acceptors bring more holes to make the concentration of the excitons increase, so that the UV emission is enhanced accordingly as shown in Figure 2.

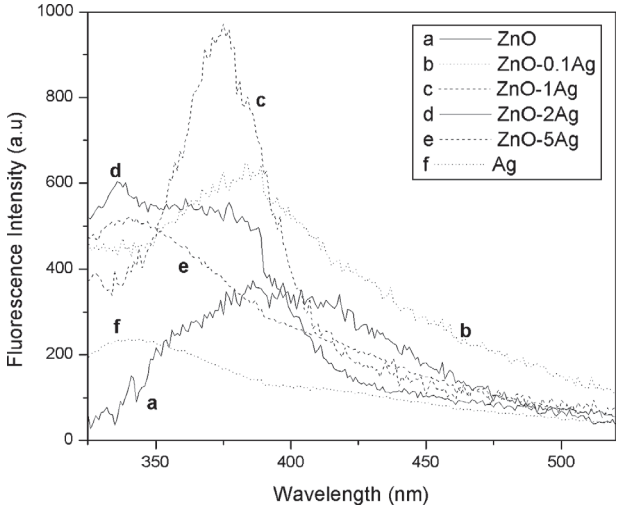

Fig. 2. Fluorescence spectra of ZnO–Ag nanocomposites.

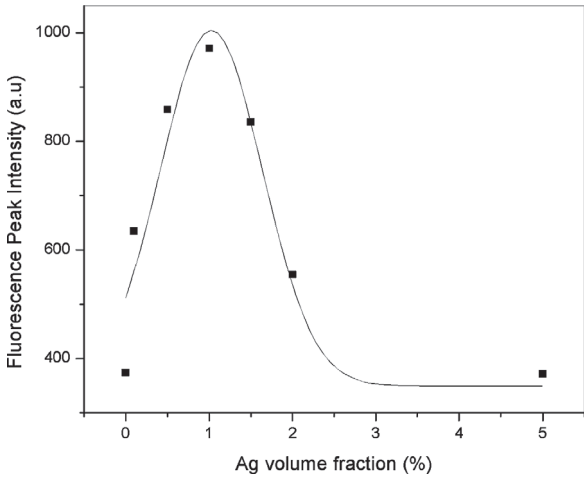

Fig. 3. The fluorescence intensity of UV peak as a function of the volume fraction of silver in ZnO–Ag nanocomposites.

Nanostructural semiconductor materials generally have more holes accumulated on its surface or in the interface than common semiconductor material.[44] Therefore, there are many holes existing in the interface between Ag nanoclusters and ZnO grains. The electrons in ZnO arrive at the interface easily because of their short mean free paths and the Coulomb forces. Based on quantum confinement effects, plenty of excitons can be formed. Then the UV emission due to exciton transition is enhanced.

The optical absorption spectroscopy and photoluminescence studies reveal the reaction mechanism at the junction. A two-fold enhancement of steady state luminescence of rhodamine 6G has been observed when it is doped with silver.[45] The presence of silver aggregates cause substantial depolarization of the luminescence and the electromagnetic interaction between Ag surface plasmons and dye molecules can result, under certain conditions, in an enhanced fluorescence quantum efficiency and photostability of the dye. The strongest UV emission of a certain ZnO–Ag film is reported to be over ten times stronger than that of a pure ZnO film and the enhancement of UV emission is caused by excitons formed at the interface between Ag nanoclusters and ZnO grains.[43] For ZnO–Ag nanocomposites, the strongest UV emission is over three times that of pure ZnO.

3.1.3. Nonlinear Optical Characterization

Figure 4 shows the nonlinear absorption of ZnO–Ag nanocomposites at a typical fluence of 300 MW/cm^2 for a wavelength of 532 nm. Interestingly, ZnO and Ag colloids show a minimum nonlinearity, while the ZnO–Ag nanocomposites clearly exhibit a larger induced absorption behavior. The nonlinear absorption coefficient increases

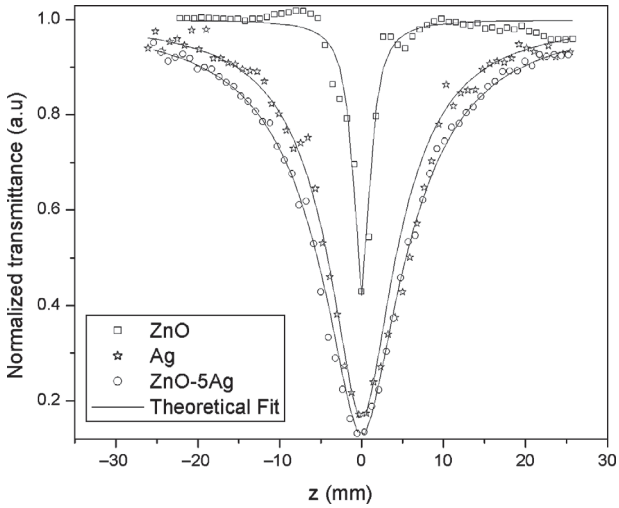

Fig. 4. Open aperture z-scan traces of ZnO–Ag nanocomposites at an intensity of 300 MW/cm^2 for an irradiation wavelength of 532 nm.

substantially in the nanocomposites, as compared to pure ZnO and Ag colloids and can be attributed to the enhancement of exciton oscillator strength. Similar increase is also reported in bimetallic and core–shell nanocomposites, as compared to pure metals.[46]

Different processes, like two photon absorption, free carrier absorption, transient absorption, interband absorption, photoejection of electrons and nonlinear scattering are reported to be operative in nanoclusters. In general, induced absorption can occur due to a variety of processes. The theory of two photon absorption process fitted well with the experimental curve infers that TPA is the basic major mechanism. The free carrier life time of ZnO is reported to be 2.8 ns.[47] Hence there is a strong possibility that the 7 ns pulses used in the present study is exciting the accumulated free carriers generated by TPA by the rising edge of the pulse. But FCA is weak compared to TPA and hence the corresponding contribution in the z-scan curves is relatively less. Silver nanoparticles are well known materials for nonlinear optical applications because of their subpicosecond time response of third-order optical nonlinearity. Transient absorption and nonlinear absorptive mechanisms are reported to lead to optical limiting in the case of Ag nanoparticles.[48]

The surface plasmon band is sensitive to laser excitation. The plasmon band of metal particles as explained on the basis of Mie theory involves dipolar oscillations of the free electrons in the conduction band that occupy energy states near the Fermi level.[1] Once these electrons are excited by a laser pulse, they do not oscillate at the same frequency as that of the unexcited electrons, thus causing the plasmon absorption band to bleach.[49] In our case, the excitation energy (532 nm or 2.3 eV) is lower than the Ag SPR (410 nm or 3.02 eV) and as such the plasmon absorption is not possible. No plasmon bleach effects are seen when the samples are excited with nanosecond laser pulses at 532 nm. Instead, a reduced transmission behavior is observed, which fits to a two photon absorption mechanism. A laser pulse can cause an intraband or interband absorption in the metal nanoparticle system, depending on the excitation wavelength and incident intensity.[50] In our case, the excitation energy (532 nm or 2.3 eV) is lower than the interband threshold from d level to p level ($E_{dp} =$ 2.5 eV), and hence interband absorption is not possible.[51] We propose that this nonlinearity is caused by two photon absorption followed by weak free carrier absorption occurring in the nanocomposites.

Figure 5 gives the closed aperture z-scan traces of ZnO–Ag nanocomposites at a fluence of 300 MW/cm^2. It is observed that the closed-aperture z-scan satisfies the condition $\Delta z \sim 1.7\ z_0$, thus confirming the presence of pure electronic third order nonlinearity.[52] The peak–valley trace in a closed aperture z-scan shows that these samples have self-defocusing (negative, $n_2 < 0$) nonlinearity, though earlier reports with picosecond pulsed lasers have shown positive nonlinearity for individual Ag nanoclusters.[53] Though laser-induced permanent sign reversal of the nonlinear refractive index is reported in Ag nanoclusters in soda-lime glass, we have not observed any such permanent effect[54] either in the intensity ranges (150–400 MW/cm^2) studied using the second harmonics of a Q-switched Nd:YAG laser or within the wavelength range 450–650 nm studied using a tunable laser (Quanta Ray MOPO, 5 ns, 10 Hz). The nanocomposites exhibit reverse saturable absorption at all wavelengths and good nonlinear absorption, which increases with increasing input intensity. The nonlinear refractive index (n_2) increases substantially in the nanocomposites, as compared to pure ZnO and Ag colloids. The dramatically enhanced nonlinear refractive response is due to the enhanced electromagnetic field existing in the interface between Ag nanoclusters and ZnO grains.[55] Since n_2 increases with absorption, thermal nonlinearity is also taken into account. It is reported that if

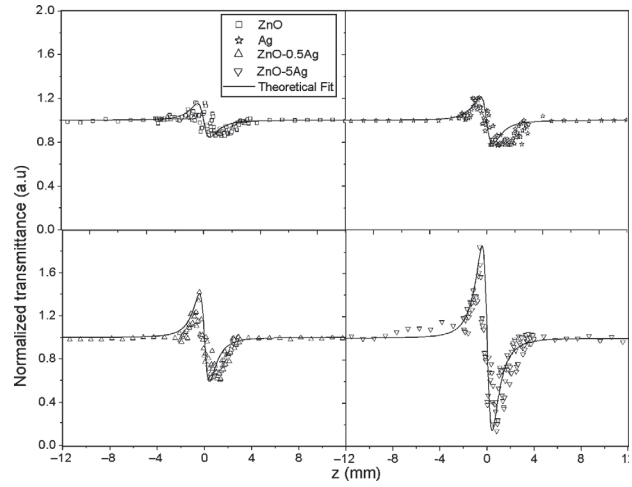

Fig. 5. Closed aperture z-scan traces of ZnO–Ag nanocomposites at an intensity of 300 MW/cm^2 for an irradiation wavelength of 532 nm.

the thermal contributions are to dominate, then there will be increase in n_2 with increase of absorption.[56]

The obtained values of nonlinear parameters of ZnO–Ag nanocomposites are given in Table I. The nonlinear refractive index of pure Ag colloid at 532 nm is reported to be of the order of 10^{-16} to 10^{-17} m^2/W. The nonlinear coefficients of Ag films are about one order of magnitude larger than that of Ag colloids.[57] It is worth noting that certain materials, such as CuO chain compounds, Ag_2S/CdS nanocomposites, organic coated quantum dots and metal clusters yielded values of order of 10^{-9} to 10^{-14} m/W for nonlinear absorption coefficient[18, 58] at a wavelength of 532 nm. These values are comparable to the values of nonlinear optical parameters obtained for nanocomposites in the present investigation. Thus, the nonlinear absorption coefficient and nonlinear refractive index measured by the z-scan technique reveals that the ZnO–Ag nanocomposites investigated in the present study have good nonlinear optical response and could be chosen as ideal candidates with potential applications in nonlinear optical devices.

3.1.4. Optical Limiting

To examine the viability of ZnO–Ag nanocomposites as optical limiters, the nonlinear transmission of the colloids are plotted as a function of input fluence derived from open aperture z-scan trace. Figure 6 illustrates the influence of volume fraction of silver in ZnO–Ag nanocomposites on the optical limiting response.

The arrow in the figure indicates the approximate fluence at which the normalized transmission begins to deviate from linearity. The optical limiting threshold is found to be high in the case of ZnO colloids (55 MW/cm^2) in comparison with that of Ag colloids (21 MW/cm^2). These values are comparable to the reported optical limiting threshold for CdS and ZnO nano colloids.[59–60] ZnO–Ag nanocomposites are found to be good optical limiters compared to ZnO and Ag and the optical limiting threshold of ZnO–5Ag nanocomposite is observed to be 12 MW/cm^2. Nanocomposites have a significant effect on the limiting performance and increasing the volume fraction of Ag reduces the limiting threshold and enhances the optical limiting performance.

Table I. Measured values of nonlinear absorption coefficient and nonlinear refractive index of ZnO–Ag nanocomposites at an intensity of 300 MW/cm^2 for an irradiation wavelength of 532 nm.

ZnO–Ag nanocomposites	β cm/GW	n_2 10^{-17} m^2/W
ZnO	20.7	−1.5
Ag	121	−2.9
ZnO–0.1Ag	138.2	−4.4
ZnO–0.5Ag	155.5	−5.9
ZnO–1Ag	172.8	−7.3
ZnO–2Ag	190.1	−11
ZnO–5Ag	207.4	−12.3

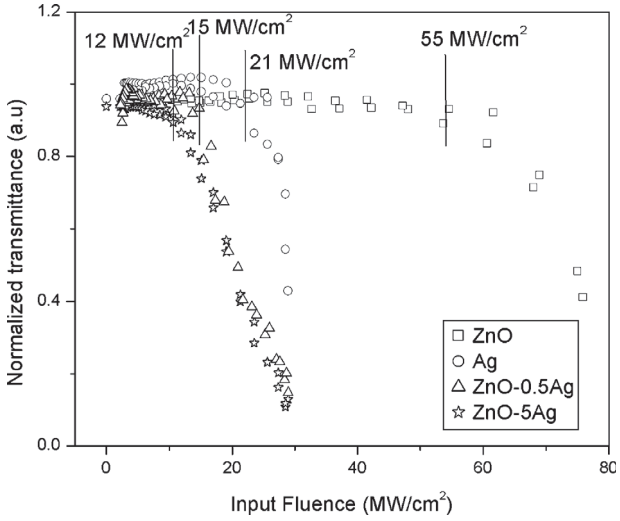

Fig. 6. Optical limiting response of ZnO–Ag nanocomposites.

3.2. ZnO–Cu

3.2.1. Absorption Spectroscopy

Figure 7 gives the room temperature absorption spectra of the ZnO–Cu nanocomposites. For copper nanocolloid, the surface plasmon absorption band (SPA) lies in the 560 nm region. The size of ZnO and Cu nanocolloids are in the range of 10–30 nm. For small volume fraction of Cu, the composite exhibits the characteristics of ZnO with a red shift in the excitonic peak. On the other hand, the ZnO–1.5Cu nanocomposite exhibits both the semiconductor and metallic behaviour. Optical absorption spectra indicate presence of well-defined ZnO excitonic feature along with the Cu surface plasmon absorption feature[40] at 545 nm. The optical absorption spectra of the clusters show a gradual shift in absorbance towards UV region, over which an extremely weak surface plasmon resonance is superposed.

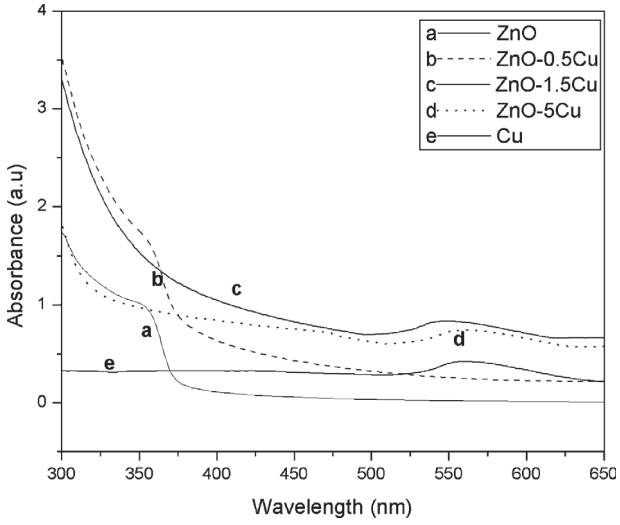

Fig. 7. Absorption spectra of ZnO–Cu nanocomposites.

When the volume fraction of Cu increases beyond 1.5%, the surface plasmon peak is shifted towards 560 nm and it has been established that the shift of the plasma band of Cu observed is a result of the accumulation of excess electrons on the ZnO/Cu particles which leads to equalization of the potentials of the conduction zones of the semiconductor and the metallic components of the nanocomposites.[42]

3.2.2. Fluorescence Spectroscopy

Photoluminescence spectra of all samples measured at room temperature are shown in Figure 8. ZnO and ZnO–0.5Cu have only emissions at 385 nm, but the intensity of the peak of ZnO–0.5Cu is much stronger than that of ZnO. ZnO–0.5Cu has the strongest UV emission which is over three times stronger than that of ZnO. It is clear that the intensity of this peak increases with the increasing amount of the Cu and Zn acceptors.

At small volume fractions, Cu acts as a sensitizer in the nanocomposites. ZnO–1Cu has UV and visible emissions. As the volume fraction of Cu increases beyond 0.5%, intensity of UV peak decreases and visible peak increases. When the ZnO colloid is overdoped by Cu, the CuO nanoclusters appears which will introduce defect states due to anion vacancies and hence there is reduction in PL intensity and increase in visible intensity.[43] ZnO–5Cu and Cu have only visible peak centered at 550 nm. It is obvious that the intensity of 550 nm peak agrees with the content of Cu nanocolloids.

At larger volume fractions of Cu in the nanocomposites, i.e., when ZnO is overdoped by Cu, defect states due to anion vacancies are introduced and hence there is ten times enhancement in visible emission compared to that of Cu. The intensity of green emission becomes stronger than that of UV emission in the composite after certain volume fraction of Cu. The intensity variation of green luminescence is systematically observed depending on the volume fraction of Cu in order to investigate the emission mechanism. This difference could be mainly because UV luminescence is degraded by excessively oxidized layer formed on the surface and the grain boundary of ZnO and Cu.[61–62]

Copper doped ZnO is a strong luminescent material and the green emission is due to copper induced levels. The transition mechanism for copper doped ZnS has been thoroughly discussed by Suzuki and Shionoya.[63] They attributed it to donor–acceptor transitions. The donor level is due to Al^{3+} used as the coactivator and acceptor levels are due to Cu^{2+} in the excited state under the UV radiation. When excited, the levels of Cu^{2+} ($3d^9$ configuration) are split into $^2t_2$ and ^2e states with $^2t_2$ lying in the higher position. In our experiments no coactivator is used so that one can rule out the presence of donor levels due to Al^{3+}. We do not observe any other impurities which would introduce donor levels. Another model to explain the green luminescence due to copper in zinc sulphide is recently proposed by Peka and Schulz.[64] Green copper luminescence in their model is due to a transition from the conduction band of ZnS to the "t_2" level of excited Cu^{2+} in the ZnS band gap.

Figure 9 shows the luminescence mechanism in ZnO–Cu nanocomposites in which the doping introduces defect levels due to anion vacancies. Impurities such as sodium, copper, lead, potassium, nickel, cadmium, iron, etc. can lead to impurity levels in the band gap and lead to luminescence.[61] Without doping, radiative transition occurs from near conduction band to the valence band. In case of Cu doped ZnO nanocomposites, enhancement of visible luminescence is due to transition from defect level to the copper induced t_2 level.

3.2.3. Nonlinear Optical Characterization

Figure 10 shows the nonlinear absorption of ZnO–Cu nanocomposites at a typical fluence of 300 MW/cm^2 for an irradiation wavelength of 532 nm. The open-aperture curve exhibits a normalized transmittance valley, indicating the presence of reverse saturable absorption in the colloids.

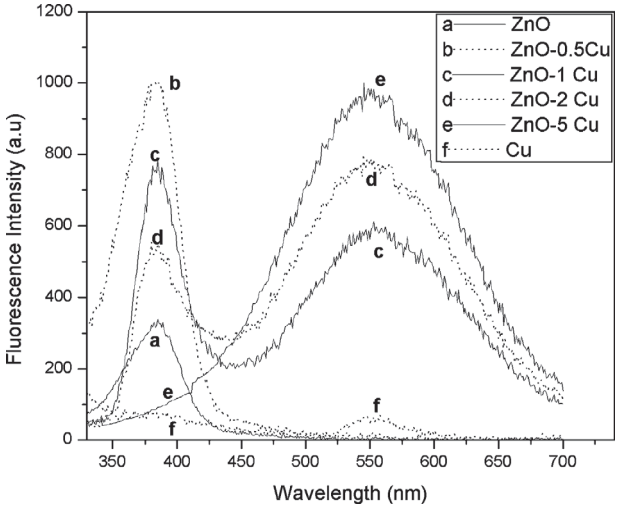

Fig. 8. Fluorescence spectra of ZnO–Cu nanocomposites.

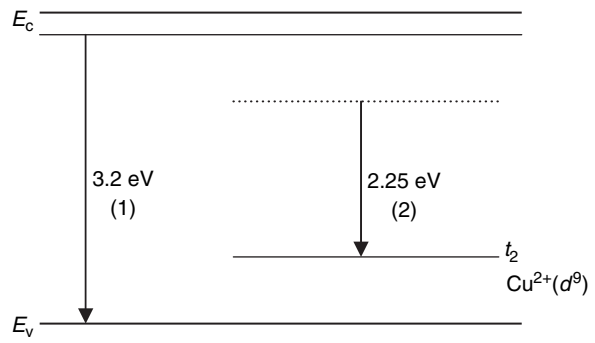

Fig. 9. Luminescence mechanism of ZnO–Cu nanocomposites, (1) transition from near conduction band edge to valence band, (2) transition from deep donor level to t_2 induced level.

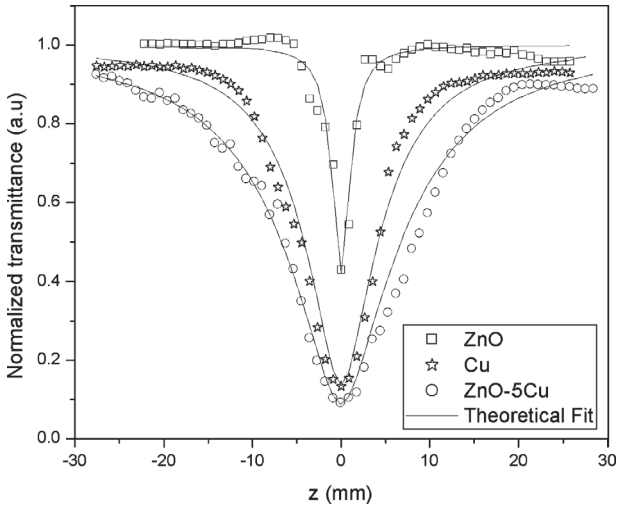

Fig. 10. Open aperture z-scan traces of ZnO–Cu nanocomposites at an intensity of 300 MW/cm^2 for an irradiation wavelength of 532 nm.

The obtained values of nonlinear absorption coefficient β at an intensity of 300 MW/cm^2 are shown in Table II.

The nonlinear absorption coefficient increases substantially in the nanocomposites, as compared to pure ZnO and Cu colloids. The theory of two photon absorption process fitted well with the experimental curve which suggests that TPA is the basic mechanism. There is the possibility of FCA, but it is weak compared to TPA and hence the corresponding contribution in the z-scan curves is relatively less.

A laser pulse can cause an intraband or interband absorption in the metal nanoparticle system, depending on the excitation wavelength and incident intensity. The electrons thus excited are free carriers possessing a whole spectrum of energies, both kinetic and potential, immediately after the absorption leading to the bleaching of the ground state plasmon band. This process is accompanied by the nascent excited state showing a transient absorption due to the free carrier absorption.[50] The possibility of photo-ejection of electrons, which is an ultrafast phenomena occurring by a two photon or multiphoton absorption process, should also be considered as a contributing factor leading to nonlinear absorption, since the excitation photons in the visible region are usually not energetic enough for monophotonic electronic ejection. In our case, the excitation energy (532 nm or 2.3 eV) is higher than the interband threshold of copper from d level to p level (571 nm $E_{dp} =$ 2.17 eV), and hence interband absorption accompanied by the absorption of free carriers generated in the conduction band is possible. Strong optical limiting properties because of interband absorption are reported in different nanoparticle systems.[51] Thus we propose that the observed nonlinearity is caused by two photon induced weak free carrier absorption and interband absorption mechanisms occurring in the nanocomposites.

Figure 11 shows the nonlinearity observed at 570 nm at a fluence of 300 MW/cm^2. An absorption saturation behavior is found in Cu colloid. However, the saturation changes over to induced absorption in all other ZnO colloids and ZnO–Cu nanocomposites. Such a change-over in the sign of the nonlinearity is related to the interplay of plasmon band bleach and optical limiting mechanisms, as found from earlier studies on metal nanoparticles in liquid and glass media.[50,65] Such behavior can generally be modeled by defining an intensity dependent nonlinear absorption coefficient $\alpha(I)$, which is a sum of independent positive and negative transmission coefficients[66]

$$\alpha(I) = \frac{\alpha}{1+(I/I_s)} + \beta I \tag{4}$$

where α is the linear absorption coefficient, β is the nonlinear absorption coefficient, and I_s is the saturation intensity.

The surface plasmon band is sensitive to laser excitation. These aspects have been addressed in several recent spectroscopic investigations.[49] Plasmon bleach effects are seen when the Cu nanocolloids are excited at its SPR with nanosecond laser pulses of 570 nm. So increased transmission behavior is observed for Cu nanocolloids, which fits to a saturable absorption mechanism. The saturation changes over to induced absorption in all the other ZnO colloids and ZnO–Cu nanocomposites. For small volume fraction of Cu, the nonlinear absorption coefficient increases substantially in the nanocomposites, as compared

Table II. Measured values of nonlinear absorption coefficient, saturation intensity and nonlinear refractive index of ZnO–Cu nanocomposites at an intensity of 300 MW/cm^2 for different irradiation wavelengths.

	Nonlinear absorption coefficient				Nonlinear refractive index
	532 nm	570 nm		650 nm	532 nm
ZnO–Cu nanocomposites	β cm/GW	β cm/GW	I_s GW/cm^2	β cm/GW	n_2 10^{-17} m^2/W
ZnO	20.7	17.3		6.7	−1.5
Cu	145.2	—	0.04	76.0	−5.9
ZnO–0.1Cu	172.8	131.3		103.7	−6.6
ZnO–0.5Cu	190.1	179.7		121.0	−7.3
ZnO–1.5Cu	248.8	138.2		145.2	−9.5
ZnO–2Cu	276.5	29.4		190.1	−11.0
ZnO–5Cu	293.8	5.4		241.9	−12.3

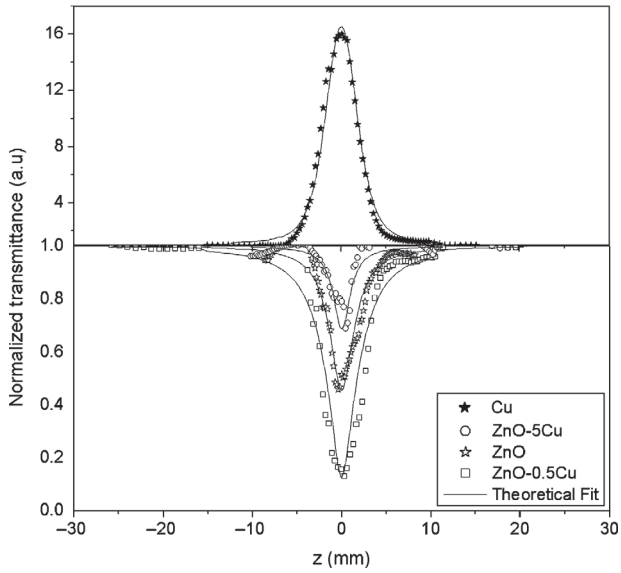

Fig. 11. Open aperture z-scan traces of ZnO–Cu nanocomposites at an intensity of 300 MW/cm^2 for an irradiation wavelength of 570 nm.

to pure ZnO. ZnO–0.5Cu exhibits maximum nonlinear absorption at 570 nm since ZnO features dominates till that composition as clearly exhibited in absorption spectra. When the volume fraction of Cu increases beyond 0.5% the nonlinear absorption coeffiencient decreases with increase in Cu composition due to the effect of plasmon bleach. Thus the nonlinearity of the ZnO–Cu nanocomposites is related to the interplay of plasmon band bleach and optical limiting mechanisms at 570 nm.

Figure 12 shows the nonlinear absorption at 650 nm. At this off-resonant excitation wavelength there is no local field enhancement within the particles, and hence the nonlinearity is less at this wavelength. Interestingly, colloids containing only Cu or ZnO nanoparticles show a minimum nonlinearity at this wavelength, while the composites clearly exhibit a larger induced absorption behavior.

Figure 13 gives the closed aperture z-scan traces of ZnO–Cu nanocomposites at a fluence of 300 MW/cm^2. It is observed that the peak–valley of closed-aperture z-scan satisfied the condition $\Delta z \sim 1.7\ z_0$, thus confirming the presence of pure electronic third order nonlinearity.[52] The peak–valley trace in a closed aperture z-scan shows that these samples have self-defocusing (negative, $n_2 < 0$) nonlinearity, though earlier reports with picosecond pulsed lasers have shown positive nonlinearity for individual Cu nanoclusters.[53] The nonlinear refractive index increases substantially in the nanocomposites, as compared to pure ZnO and Cu colloids. The enhanced nonlinear refractive response is due to the enhanced electromagnetic field existing in the interface between Cu nanoclusters and ZnO grains.[55] Since n_2 increases with absorption, thermal nonlinearity is also taken into account.[56]

The obtained values of nonlinear parameters of ZnO–Cu nanocomposites are given in Table II. The nonlinear absorption coeffiecient of CuO chain compounds and metal clusters yielded values of order of 10^{-9} to 10^{-14} m/W for nonlinear absorption coefficient at a wavelength of 532 nm.[18,58] These values are comparable to the values of nonlinear optical parameters obtained for nanocomposites in the present investigation.

3.2.4. Optical Limiting

Figure 14 illustrates the influence of volume fraction of copper in ZnO–Cu nanocomposites on the optical limiting response. The optical limiting threshold is found to be high in the case of ZnO colloids (55 MW/cm^2) in comparison with the Cu colloids (10 MW/cm^2). ZnO–Cu nanocomposites are found to be good optical limiters compared to ZnO and Cu and the optical limiting threshold of ZnO–5Cu

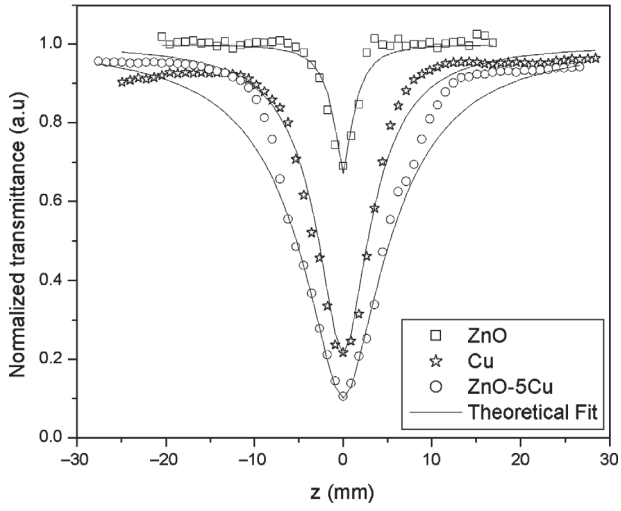

Fig. 12. Open aperture z-scan traces of ZnO–Cu nanocomposites at an intensity of 300 MW/cm^2 for an irradiation wavelength of 650 nm.

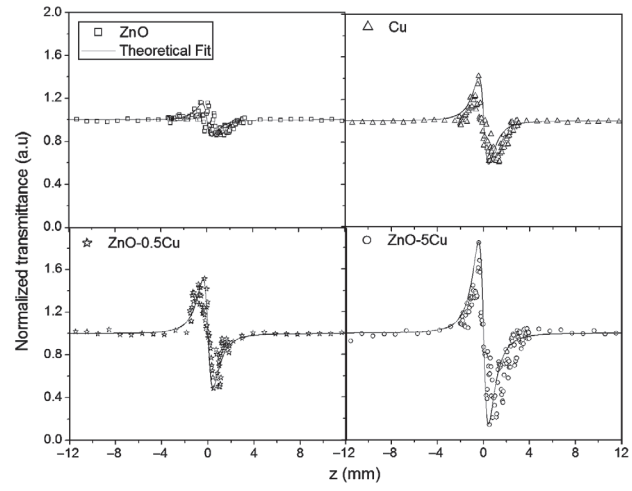

Fig. 13. Closed aperture z-scan traces of ZnO–Cu nanocomposites at an intensity of 300 MW/cm^2 for an irradiation wavelength of 532 nm.

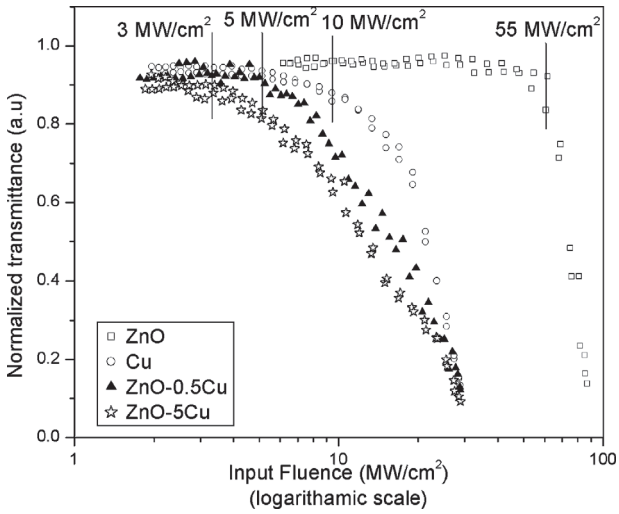

Fig. 14. Optical limiting response of ZnO–Cu nanocomposites.

nanocomposites is observed to be 3 MW/cm^2. Nanocomposites have a significant effect on the limiting performance and increasing the volume fraction of Cu reduces the limiting threshold and enhances the optical limiting performance.

3.3. ZnO–CdS

3.3.1. Absorption Spectroscopy

Figure 15 gives the room temperature absorption spectra of the ZnO–CdS nanocomposites. The excitonic peak of ZnO and that of CdS colloids are found to be blue shifted with respect to their bulk which could be attributed to the confinement effects.[39, 67] From the shift of absorption edge, the size of ZnO and CdS nanocolloids are calculated to be in the range of 10–12 nm. The presence of excitonic peak itself indicates that the composites are of nanometer

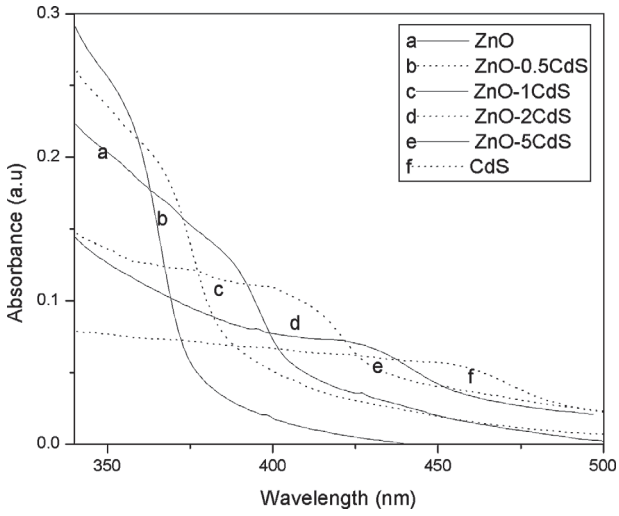

Fig. 15. Absorption spectra of ZnO–CdS nanocomposites.

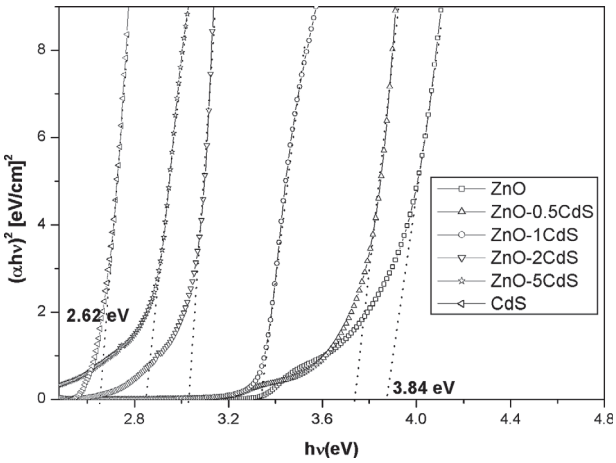

Fig. 16. Optical band gap of ZnO–CdS nanocomposites.

size. It is seen that the absorption edge corresponding to the nanocomposites gets red shifted as a function of the CdS content.

3.3.2. Optical Bandgap

The direct bandgap of ZnO–CdS nanocomposites is estimated from the graph of $h\nu$ versus $(\alpha h\nu)^2$. The optical band gap (E_g) is found to be dependent on the composition and there is a decrease in the band gap of the semiconductor with an increase in the volume fraction of CdS in the nanocomposites as shown in Figure 16. E_g changes from 3.84 eV for ZnO to 2.62 eV for CdS almost in proportion to the composition of CdS. Within the range of compositions studied, the optical bandgap is tunable from 2.62 eV to 3.84 eV. The bandgap engineering in ZnS–CdS is reported to be from 2.58 to 3.91 eV.[68]

3.3.3. Fluorescence Spectroscopy

Photoluminescence spectra of all the samples measured at room temperature are shown in Figure 17. The 385 nm emission is the near band edge emission of ZnO and the

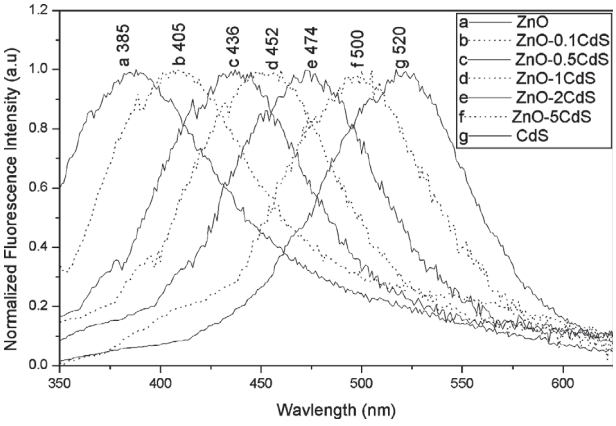

Fig. 17. Fluorescence spectra of ZnO–CdS nanocomposites.

520 nm emission is the near band edge emission peak of CdS. Emission peaks of ZnO–CdS nanocomposites changes from 385 nm to 520 nm almost in proportion to changes in E_g. It is possible to obtain a desired luminescence colour from UV to green by simply adjusting the composition. The tuning of luminescence in ZnS–CdS is reported to be from blue to red in proportion to change in E_g.[68]

3.3.4. Nonlinear Optical Characterization

Figure 18 shows the nonlinear absorption of ZnO–CdS nanocomposites at a typical fluence of 300 MW/cm^2 for an irradiation wavelength of 532 nm. The obtained nonlinearity is found to be of the third order, as it fits to a two photon absorption (TPA) process. The nonlinear absorption coefficient increases substantially in the nanocomposites, as compared to pure ZnO and CdS colloids due to the enhancement of exciton oscillator strength.[12] The larger nonlinear absorption in semiconductors such as ZnSe, ZnO, and ZnS is reported to be due to two photon induced free carrier absorption along with TPA.[47] The enhancement of nonlinear absorption in Ag_2S–CdS nanocomposites in comparison with the CdS nanoparticles is reported to be due to free carrier absorption and the free carrier life time of ZnO is determined to be a few nanoseconds.[18] Thus we propose that the observed nonlinearity is caused by two photon absorption followed by weak free carrier absorption in the nanocomposites.

Figure 19 shows the nonlinearity observed for 450 nm at a fluence of 300 MW/cm^2. An absorption saturation behavior is found in CdS colloid and ZnO–5CdS nanocomposites. However, all the other ZnO colloids and ZnO–CdS nanocomposites exhibit induced absorption at this wavelength. Such a change-over in the sign of the nonlinearity is related to the interplay of exciton band bleach and optical limiting mechanisms, as found from earlier studies of semiconductor nanoparticles.[69]

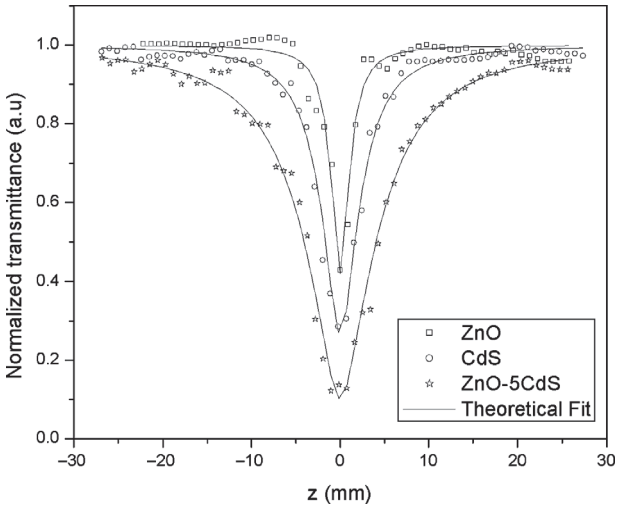

Fig. 18. Open aperture z-scan traces of ZnO–CdS nanocomposites at an intensity of 300 MW/cm^2 for an irradiation wavelength of 532 nm.

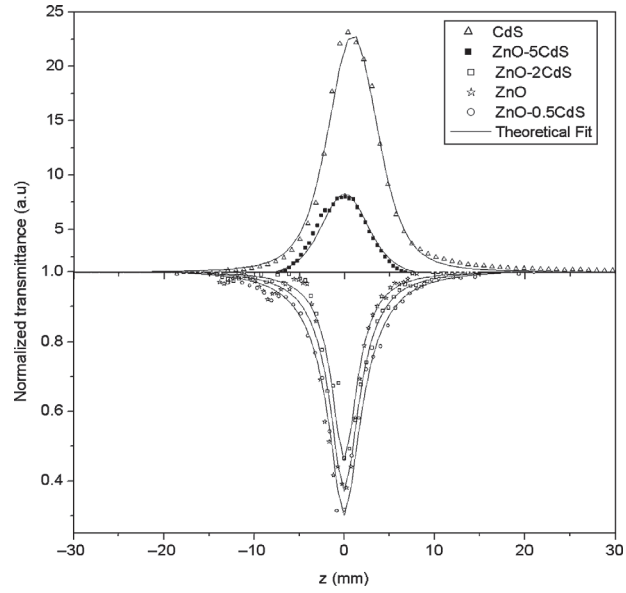

Fig. 19. Open aperture z-scan traces of ZnO–CdS nanocomposites at an intensity of 300 MW/cm^2 for an irradiation wavelength of 450 nm.

The excitonic peak is sensitive to laser excitation. As the particle size is reduced, a series of nearby transitions occurring at slightly different energies in the bulk are compressed by quantum confinement into a single, intense transition in a quantum dot. Therefore, the oscillator strength of the nanoparticle is concentrated into just a few transitions and the strong exciton bleaching can be expected. Exciton bleach effects are seen when the CdS nanocolloids are excited at excitonic resonance with nanosecond laser pulses of 450 nm. So increased transmission behavior is observed for CdS nanocolloids, which fits to a saturable absorption mechanism. On the other hand, ZnO colloids exhibit induced absorption at this wavelength. For small volume fraction of CdS, the nonlinear absorption coefficient increases substantially in the nanocomposites, as compared to pure ZnO. ZnO–0.5CdS exhibits maximum nonlinear absorption at 450 nm and can be attributed to the enhancement of exciton oscillator strength.[12] When the volume fraction of CdS increases beyond 0.5% the nonlinear absorption coeffiencient decreases with increase in the volume fraction of CdS and it becomes a saturable absorber at and above 5% CdS due to the interplay of exciton bleach and optical limiting mechanisms. The excitonic bleaching of the CdS nanocolloids originates from the transition between the ground state $1S(e)$ and the lowest excited state $1S_{3/2}(h)$ since the excitation at 450 nm corresponds to the absorption close to the resonance of the $1S(e)$–$1S_{3/2}(h)$ excitonic transition.[69] Thus the nonlinearity of the ZnO–CdS nanocomposites is related to the interplay of exciton bleach and optical limiting mechanisms at 450 nm. The great potential of using the ZnO–CdS nanocomposite lies in the fact that

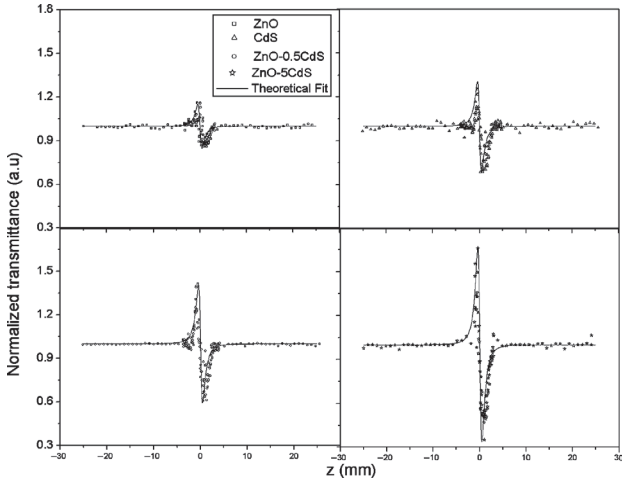

Fig. 20. Closed aperture z-scan traces of ZnO–CdS nanocomposites at an intensity of 300 MW/cm^2 for an irradiation wavelength of 532 nm.

the composition of the constituent elements can be readily altered to optimize the desired NLO properties either as a saturable absorber or as a reverse saturable absorber.

Figure 20 gives the closed aperture z-scan traces of ZnO–CdS nanocomposites at a fluence of 300 MW/cm^2. It is observed that the peak–valley of closed-aperture z-scan satisfied the condition $\Delta z \sim 1.7\ z_0$, thus confirming the presence of pure electronic third order nonlinearity.[52] The peak–valley trace in a closed aperture z-scan shows that these samples have self-defocusing (negative, $n_2 < 0$) nonlinearity, though earlier reports have shown positive nonlinearity for individual CdS nanoclusters prepared by laser ablation.[70] The nonlinear refractive index increases substantially in the nanocomposites, as compared to pure ZnO and CdS colloids and can be attributed to the enhancement of exciton oscillator strength.[12] Since n_2 increases with absorption, thermal nonlinearity is also taken into account.[56]

The obtained values of nonlinear optical parameters of ZnO–CdS nanocomposites are given in Table III. The nonlinear refractive index of the pure semiconductor nano colloids at 532 nm are reported to be of the order of 10^{-16} to 10^{-17} m^2/W. The third order nonlinear absorption coefficient of CdS nanocrystals are reported to be of the order of 10^{-10} m/W.[71] Ag_2S–CdS nanocomposites yielded values of order of 10^{-9} to 10^{-14} m/W for nonlinear absorption coefficient at a wavelength of 532 nm.[18, 58] These values are comparable to the values of nonlinear optical parameters obtained for nanocomposites in the present investigation.

Table III. Measured values of nonlinear absorption coefficient, saturation intensity and nonlinear refractive index of ZnO–CdS nanocomposites at an intensity of 300 MW/cm^2 for different irradiation wavelengths.

	Nonlinear absorption coefficient			Nonlinear refractive index
	450 nm		532 nm	532 nm
ZnO–CdS nanocomposites	β cm/GW	I_s GW/cm^2	β cm/GW	n_2 10^{-17} m^2/W
ZnO	51.8		20.7	−1.5
CdS		0.20	51.8	−4.4
ZnO–0.5CdS	131.3		62.2	−5.9
ZnO–1CdS	34.6		155.5	−6.9
ZnO–2CdS	17.3		207.4	−8.9
ZnO–5CdS		0.04	242.0	−11.0

3.3.5. Optical Limiting

Figure 21 illustrates the influence of volume fraction of CdS in ZnO–CdS nanocomposites on the optical limiting response. The optical limiting threshold is found to be high in the case of ZnO colloids (55 MW/cm^2) in comparison with the CdS colloids (20 MW/cm^2). ZnO–CdS nanocomposites are found to be good optical limiters compared to ZnO and CdS and the optical limiting threshold of ZnO–5CdS nanocomposites is observed to be 7 MW/cm^2. Nanocomposites have a significant effect on the limiting performance and increasing the volume fraction of CdS reduces the limiting threshold and enhances the optical limiting performance.

3.4. ZnO–TiO_2

3.4.1. Absorption Spectroscopy

Figure 22 gives the room temperature absorption spectra of the ZnO–TiO_2 nanocomposites. The excitonic peak of ZnO and that of TiO_2 colloids are found to be blue shifted with respect to their bulk which could be attributed to the confinement effects.[39, 72] From the shift of the absorption band edge, the size of ZnO and TiO_2 nanocolloids are calculated to be in the range of 8–10 nm. The presence of excitonic peak itself indicates that the composites are of nanometer size. It is seen that the absorption edge

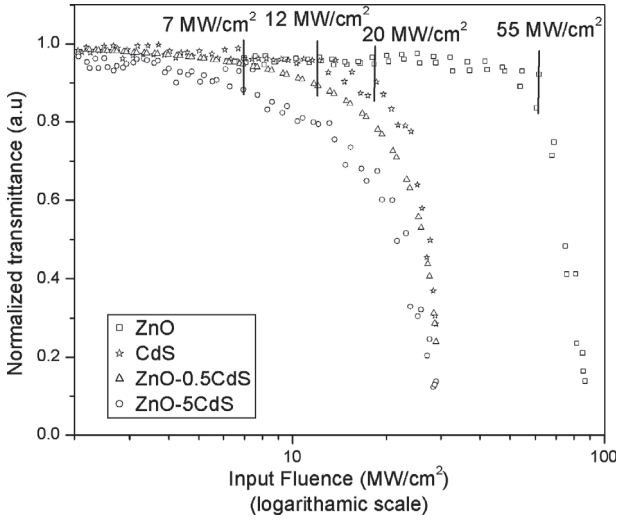

Fig. 21. Optical limiting response of ZnO–CdS nanocomposites at 532 nm.

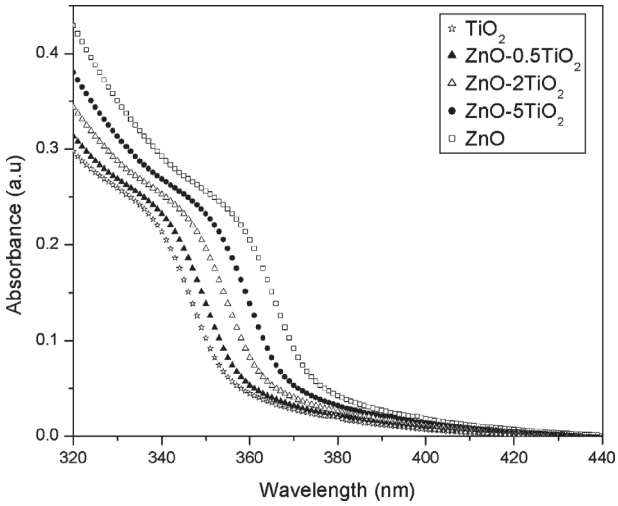

Fig. 22. Absorption spectra of ZnO–TiO_2 nanocomposites.

corresponding to the nanocomposites gets red shifted as a function of the TiO_2 content compared to pure TiO_2.

3.4.2. Optical Bandgap

The direct bandgap of ZnO–TiO_2 nanocomposites is estimated from the graph of $h\nu$ versus $(\alpha h\nu)^2$. The optical band gap (E_g) is found to be dependent on the composition and there is a decrease in the band gap of the nanocomposite with an increase in volume fraction of TiO_2 compared to pure TiO_2 as shown in Figure 23. This is because higher carrier concentrations in conduction and valence bands lead to bandgap reduction due to enhanced carrier–carrier interaction as well as by the distortion of the crystal lattice since the optical properties of the nano colloids strongly depend on the micro-structure of the materials. Both bandgap narrowing mechanisms add up and they are oftern hard to separate.[23] E_g changes from 3.84 eV to 4.12 eV almost in proportion to the composition of TiO_2.

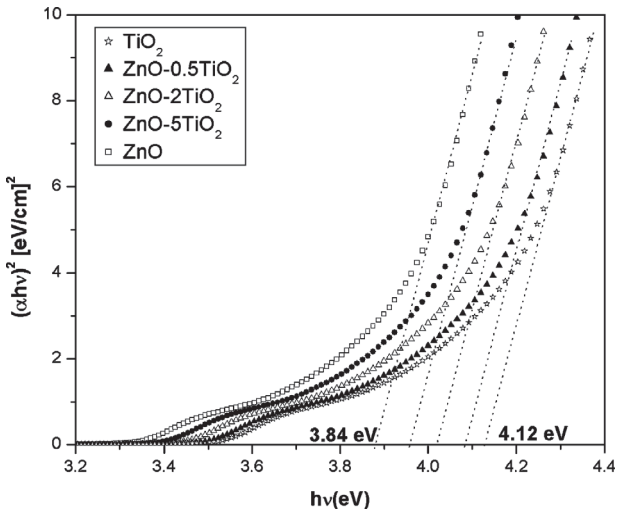

Fig. 23. Optical band gap of ZnO–TiO_2 nanocomposites.

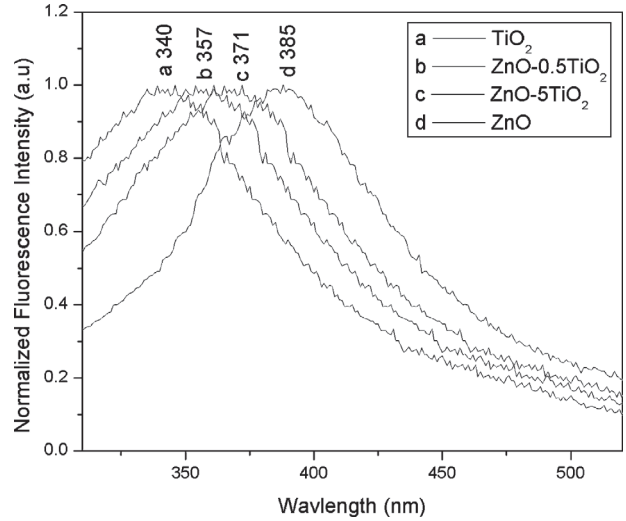

Fig. 24. Fluorescence spectra of ZnO–TiO_2 nanocomposites.

3.4.3. Fluorescence Spectroscopy

Photoluminescence spectra of all samples for an excitation wavelength of 300 nm measured at room temperature are shown in Figure 24. The 385 nm emission is the near band edge emission of ZnO and the 340 nm emission is the near band edge emission peak of TiO_2. Emission peaks of ZnO–TiO_2 nanocomposites changes from 340 nm to 385 nm almost in proportion to changes in E_g. It is possible to obtain a desired wavelength of UV luminescence by simply adjusting the composition.

3.4.4. Nonlinear Optical Characterization

Figure 25 shows the nonlinear absorption of ZnO–TiO_2 nanocomposites at a typical fluence of 300 MW/cm^2 for an irradiation wavelength of 532 nm. ZnO and

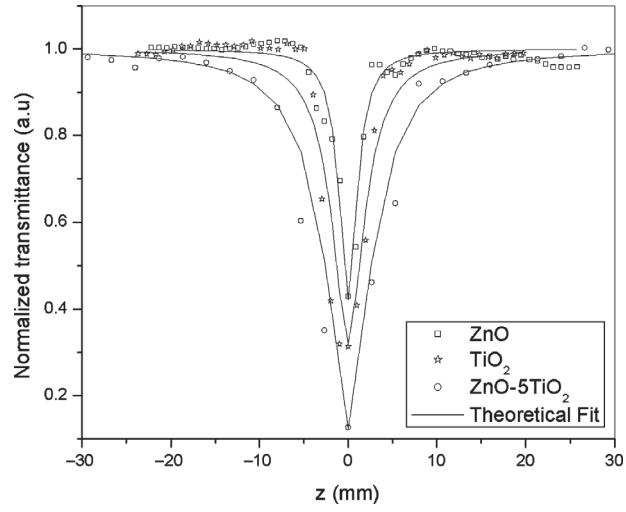

Fig. 25. Open aperture z-scan traces of ZnO–TiO_2 nanocomposites at an intensity of 300 MW/cm^2 for an irradiation wavelength of 532 nm.

TiO_2 colloids show a minimum nonlinearity, while the ZnO–TiO_2 nanocomposites clearly exhibit a larger induced absorption behavior and can be attributed to the enhancement of exciton oscillator strength.[12] The obtained nonlinearity is found to be of the third order, as it fits to a two photon absorption (TPA) process. The nanosecond pulses can excite the accumulated free carriers generated by TPA in ZnO. But the free carrier absorption is weak compared to TPA and hence the corresponding contribution in the z-scan curves is relatively less. The large optical nonlinearities in the nanosized particles containing TiO_2 are reported to be due to TPA.[73] Thus we propose that the observed nonlinearity is caused by two photon absorption followed by weak free carrier absorption in the nanocomposites.

Figure 26 gives the closed aperture z-scan traces of ZnO–TiO_2 nanocomposites at a fluence of 300 MW/cm^2. It is observed that the peak–valley of closed-aperture z-scan satisfied the condition $\Delta z \sim 1.7\ z_0$, thus confirming the presence of pure electronic third order nonlinearity.[52] The peak–valley trace in a closed aperture z-scan shows that these samples have self-defocusing (negative, $n_2 < 0$) nonlinearity, though earlier reports with 780 nm picosecond pulsed lasers have shown positive nonlinearity for PMMA-TiO_2 nanocomposites.[74] The nonlinear refractive index increases substantially in the nanocomposites, as compared to pure ZnO and TiO_2 colloids and can be attributed to the enhancement of exciton oscillator strength.[12] Since n_2 increases with absorption, thermal nonlinearity is also taken into account.[56]

The obtained values of nonlinear optical parameters of ZnO–TiO_2 nanocomposites are shown in Table IV. The third order optical nonlinearity, n_2 of TiO_2 nanocrystalline particles dispersed in SiO_2 is found to be 10^{-12} esu at 532 nm with nanosecond laser pulses.[75] The two photon absorption coefficient of TiO_2 nanocrystal is reported to be 14 cm/GW at 532 nm and these values are comparable to the value of β obtained for nanocomposites in the present investigation.[75] Thus, the nonlinear absorption coefficient and nonlinear refractive index measured by the z-scan technique reveals that the ZnO–TiO_2 nanocomposites investigated in the present study have good nonlinear optical response and could be chosen as ideal candidates with potential applications in nonlinear optics.

Table IV. Measured values of nonlinear absorption coefficient and nonlinear refractive index of ZnO–TiO_2 nanocomposites at an intensity of 300 MW/cm^2 for an irradiation wavelength of 532 nm.

ZnO–TiO_2 nanocomposites	β cm/GW	n_2 10^{-17} m^2/W
ZnO	20.7	−1.5
TiO_2	77.8	−2.9
ZnO–0.1TiO_2	86.4	−4.1
ZnO–0.5TiO_2	100.2	−6.0
ZnO–1TiO_2	121.0	−6.9
ZnO–2TiO_2	138.2	−8.9
ZnO–5TiO_2	180.0	−10.3

3.4.5. Optical Limiting

Figure 27 illustrates the influence of volume fraction of TiO_2 in ZnO–TiO_2 nanocomposites on the optical limiting response. The optical limiting threshold is found to be high in the case of ZnO colloids (55 MW/cm^2) in comparison with the TiO_2 colloids (22 MW/cm^2). ZnO–TiO_2 nanocomposites are found to be good optical limiters compared to ZnO and TiO_2 and the optical limiting threshold of ZnO–5TiO_2 nanocomposites is observed to be 13 MW/cm^2. Nanocomposites have a significant effect on the limiting performance and increasing the volume fraction of TiO_2 reduces the limiting threshold and enhances the optical limiting performance.

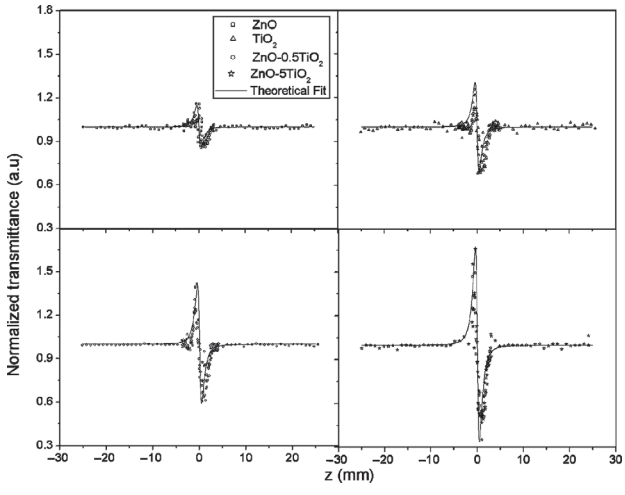

Fig. 26. Closed aperture z-scan traces of ZnO–TiO_2 nanocomposites at an intensity of 300 MW/cm^2 for an irradiation wavelength of 532 nm.

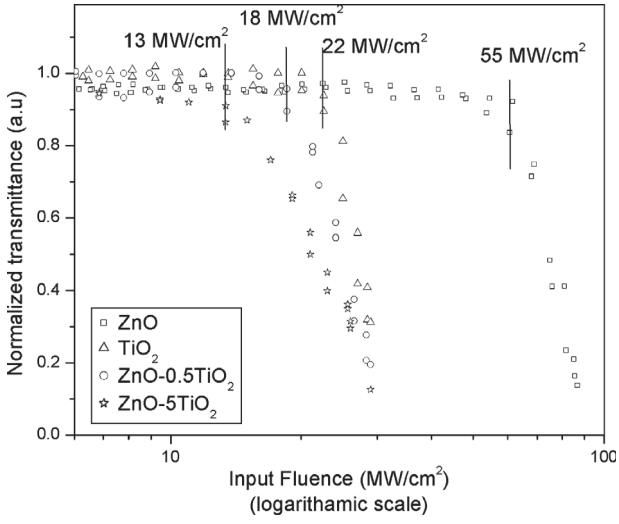

Fig. 27. Optical limiting response of ZnO–TiO_2 nanocomposites.

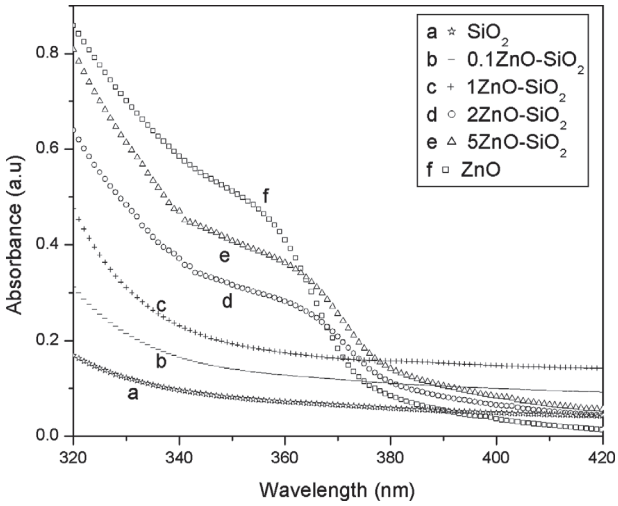

Fig. 28. Absorption spectra of ZnO–SiO_2 nanocomposites.

3.5. ZnO–SiO_2

3.5.1. Absorption Spectroscopy

Figure 28 gives the room temperature absorption spectra of the ZnO–SiO_2 nanocomposites. The excitonic peak of ZnO colloid is found to be blue shifted with respect to that of bulk ZnO which could be attributed to the confinement effects.[39] There is a change in absorption with the ZnO content and as the volume fraction of ZnO increases beyond 2%, the excitonic peak exhibits its signature. It is seen that the absorption edge corresponding to the nanocomposites gets red shifted and the exciton oscillator strength increases as a function of the ZnO content consistent with published reports.[74]

3.5.2. Fluorescence Spectroscopy

Photoluminescence spectra of all the samples measured at room temperature are shown in Figure 29. The intensities of the emission peaks depend on the volume fraction of ZnO present in the samples. ZnO and ZnO–SiO_2 composites exhibit emission at 385 nm, but the fluorescence intensity of the composites is much stronger than that of ZnO. 1ZnO–SiO_2 has the strongest UV emission centered at 385 nm. The increase of the UV emission can be attributed to the enhancement of the exciton oscillator strength.[12]

Figure 30 shows the PL intensity as a function of the ZnO content. It is clear that the intensity of this peak increases with the increasing amount of the Zn acceptors. As the volume fraction of ZnO increases, the formation of aggregates decreases the fluorescence emission.[76] This can be related to the phenomenon of re-absorption and emission at higher concentrations which ultimately reduces the fluorescence emission. As the volume fraction increases, the low frequency tail of the absorption spectrum of the sample overlaps with the high frequency end of its fluorescence spectrum. The fluorescence from the excited state is reabsorbed by the ground state. This process increases with increase in volume fraction, which results in decrease of fluorescence. The formation of aggregates quenches the fluorescence emission by collision or long range non-radiative energy transfer. The emission of ZnO at 385 nm can be attributed to exciton transition. As the volume fraction of ZnO increases, the exciton oscillator strength increases, so that the UV emission is enhanced accordingly as shown in Figure 29. Nanostructural semiconductor materials generally have more holes accumulated on its surface or in the interface than common semiconductor materials.[44]

3.5.3. Nonlinear Optical Characterization

Figure 31 shows the nonlinear absorption of ZnO–SiO_2 nanocomposites at a typical fluence of 300 MW/cm^2. The nonlinear absorption coefficient increases substantially in

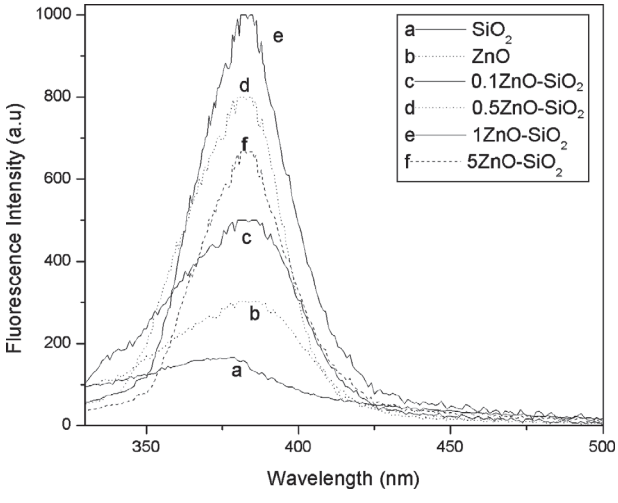

Fig. 29. Fluorescence spectra of ZnO–SiO_2 nanocomposites.

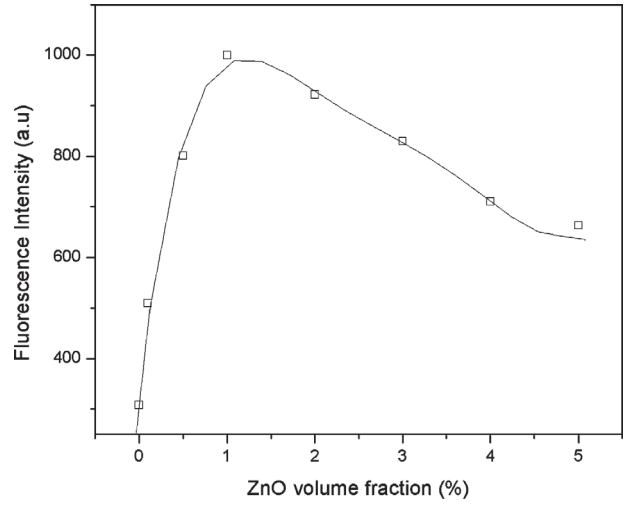

Fig. 30. The fluorescence intensity of UV peak as a function of the volume fraction of ZnO in ZnO–SiO_2 nanocomposites.

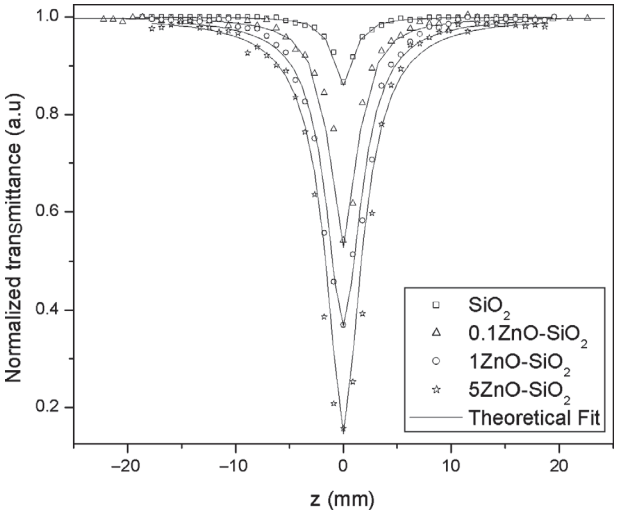

Fig. 31. Open aperture z-scan traces of ZnO–SiO_2 nanocomposites at an intensity of 300 MW/cm^2 for an irradiation wavelength of 532 nm.

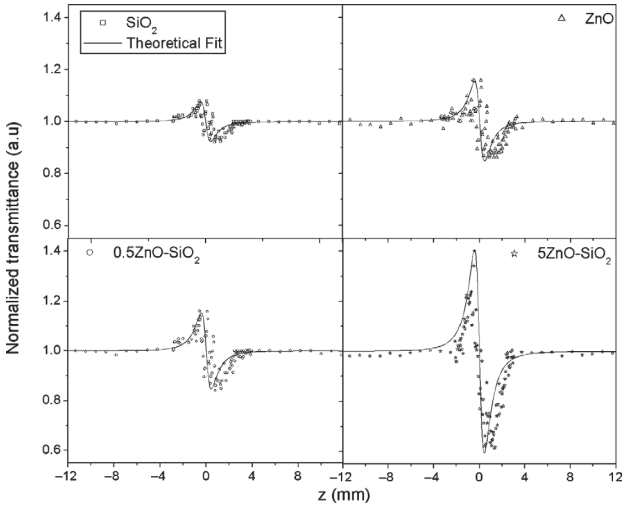

Fig. 32. Closed aperture z-scan traces of ZnO–SiO_2 nanocomposites at an intensity of 300 MW/cm^2 for an irradiation wavelength of 532 nm.

the nanocomposites, as compared to pure ZnO and SiO_2 colloids. It is reported that the nonlinear absorption coefficient increases in the core–shell silica nanocomposites, as compared to pure nanoparticles.[46] The large values of the third-order nonlinearity can be attributed to the enhancement of exciton oscillator strength.[12]

The obtained nonlinearity is found to be of the third order, as it fits to a two photon absorption process. The nanosecond pulses can excite the accumulated free carriers generated by TPA in ZnO. But the free carrier absorption is weak compared to TPA and hence the corresponding contribution in the z-scan curves is relatively less. It is possible that nonlinear scattering dominates two photon absorption on the silica colloids and the presence of nonlinear scattering reduces the two photon absorption coeffiecient in silica colloids.[77] Both the linear and the nonlinear absorption of wide-band silica colloids in the visible and the near-infrared ranges are known to be negligible if the input intensity is well below the breakdown threshold.[77] Therefore, two-photon absorption contribution is expected to be very small in silica colloids because the total input intensity is relatively small compared to the breakdown threshold. Hence we propose that the nonlinearity in ZnO–SiO_2 nanocomposites is caused by two photon absorption followed by weak free carrier absorption and nonlinear scattering.

Figure 32 gives the closed aperture z-scan traces of ZnO–SiO_2 nanocomposites at a fluence of 300 MW/cm^2. The closed-aperture curve exhibits a peak–valley shape, indicating a negative value of the nonlinear refractive index n_2. It is observed that the peak–valley of closed-aperture z-scan satisfied the condition $\Delta z \sim 1.7\ z_0$, thus confirming the presence of pure electronic third order nonlinearity.[52] The peak–valley trace in a closed aperture z-scan shows that these samples have self-defocusing (negative, $n_2 < 0$) nonlinearity, though earlier reports with nanosecond pulsed lasers have shown positive nonlinearity for fused silica due to the mechanism of electrostriction.[78]

We suggest that the possible physical origin of the nonlinear refraction of ZnO–SiO_2 composites is mainly a two photon absorption process and partially nonlinear scattering and weak thermal effects in the nanosecond time domain. It is reported that the difference between the third-order optical susceptibilities for z-scan and four wave mixing (FWM) is due to scattering from the surface of silica nanoaerogels in the z-scan measurements.[24] We have not observed any sign reversal of the nonlinear refractive index either in the intensity ranges (150–400 MW/cm^2) studied using the second harmonics of a Q-switched Nd:YAG laser or within the wavelength range 450–650 nm studied using a tunable laser (Quanta Ray MOPO, 5 ns, 10 Hz). The nanocomposites exhibit induced absorption at all wavelengths and good nonlinear absorption, which increases with increase in input intensity. The nonlinear refractive index increases substantially in the nanocomposites, as compared to pure ZnO and SiO_2 colloids. The large enhancement of the third-order nonlinearity of the silica aerogel is reported to be due to the quantum confinement effect of bound electrons, which is induced by the nanostructure nature of the sample.[79]

In the present investigations, the obtained values of nonlinear optical parameters of ZnO–SiO_2 nanocomposites are shown in Table V. The third-order nonlinear susceptibility of silica nanoaerogels is estimated to be 9.6×10^{-19} m^2/V^2 (6.9×10^{-11} esu) from FWM measurements.[79] In the case of fused silica, the nonlinear refractive index is reported to be quite small, roughly 3×10^{-20} m^2/W, which is about two order of magnitude below the nonlinear refractive index of most of the materials usually studied with the z-scan method.[79] The core–shell silica nanocomposites yielded values of the order of 10^{-9} to 10^{-14} m/W for nonlinear absorption coefficient and 10^{-16} to 10^{-20} m^2/W

Table V. Measured values of nonlinear absorption coefficient and nonlinear refractive index of ZnO–SiO_2 nanocomposites at an intensity of 300 MW/cm^2 for an irradiation wavelength of 532 nm.

ZnO–SiO_2 nanocomposites	β cm/GW	n_2 10^{-17} m^2/W
ZnO	20.7	−1.5
SiO_2	1.7	−0.9
0.1ZnO–SiO_2	12.1	−2.2
0.5ZnO–SiO_2	27.7	−3.1
1ZnO–SiO_2	41.5	−4.4
2ZnO–SiO_2	86.4	−5.0
5ZnO–SiO_2	138.2	−5.9

for nonlinear refractive index at a wavelength of 532 nm. These values are comparable to the value of β and n_2 obtained for nanocomposites in the present investigation.

3.5.4. Optical Limiting

Figure 33 illustrates the influence of volume fraction of ZnO in ZnO–SiO_2 nanocomposites on the optical limiting response. The optical limiting threshold is found to be very low in the case of ZnO colloids (55 MW/cm^2) in comparison with that of the silica colloids (120 MW/cm^2). ZnO–SiO_2 nanocomposites are found to be good optical limiters compared to ZnO and SiO_2 and the optical limiting threshold of 5ZnO–SiO_2 nanocomposites is observed to be 20 MW/cm^2. Nanocomposites have a significant effect on the limiting performance and increasing the volume fraction of ZnO reduces the limiting threshold and enhances the optical limiting performance.

3.6. ZnO–TiO_2–SiO_2

3.6.1. Absorption Spectroscopy

Figure 34 gives the room temperature absorption spectra of the ZnO–TiO_2–SiO_2 nanocomposites. There is a change

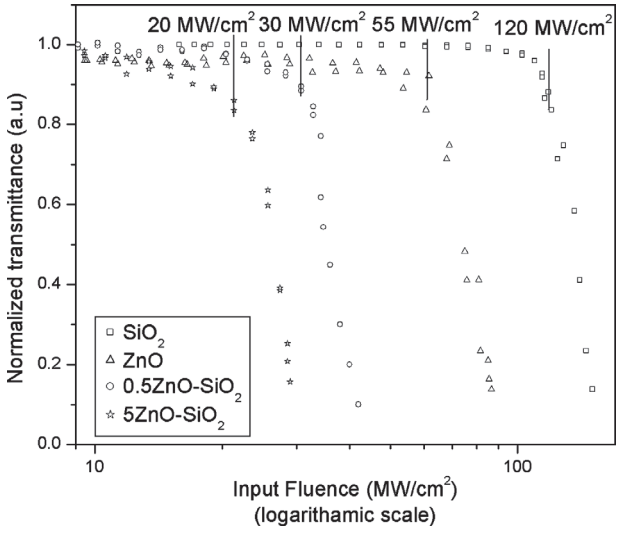

Fig. 33. Optical limiting response of ZnO–SiO_2 nanocomposites generated from open aperture z-scan traces at 532 nm.

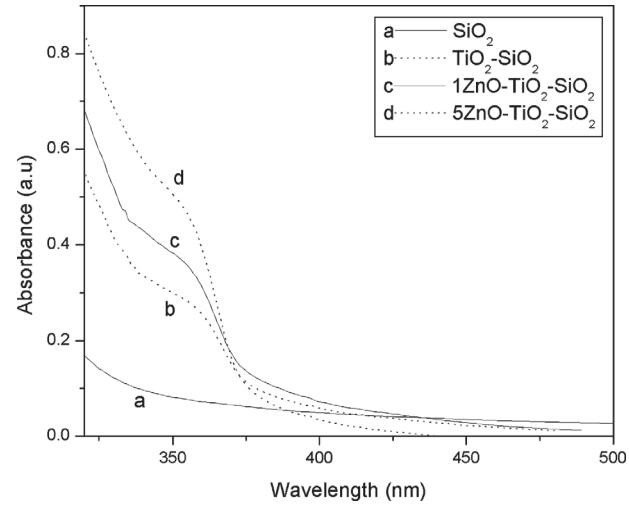

Fig. 34. Absorption spectra of ZnO–TiO_2–SiO_2 nanocomposites.

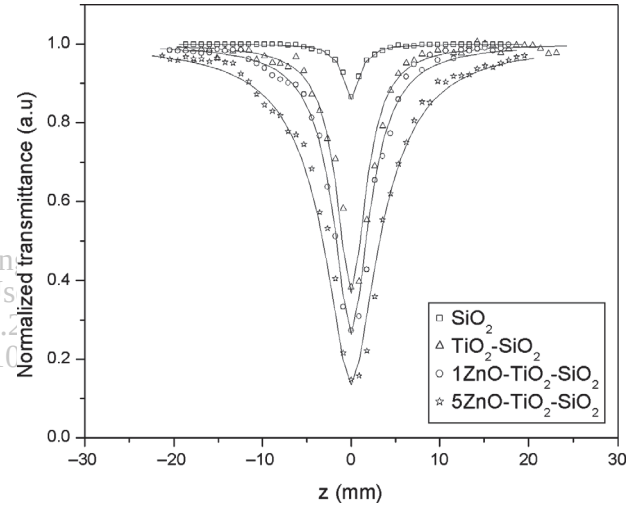

Fig. 35. Open aperture z-scan traces of ZnO–TiO_2–SiO_2 nanocomposites [intensity of 300 MW/cm^2, wavelength = 532 nm].

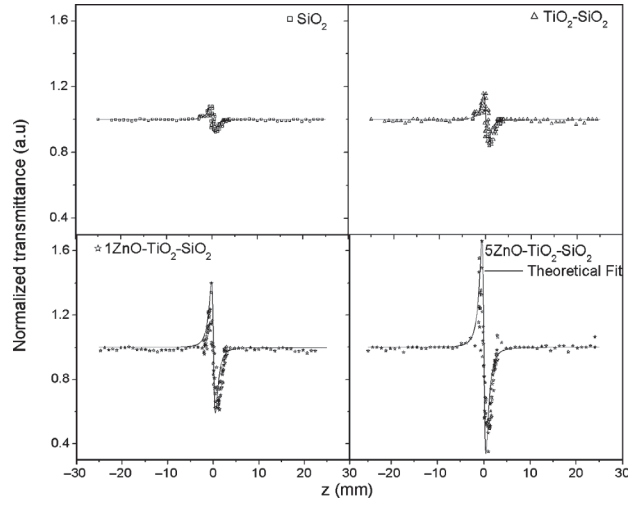

Fig. 36. Closed aperture z-scan traces of ZnO–TiO_2–SiO_2 nanocomposites [I = 300 MW/cm^2, irradiation wavelength = 532 nm].

Table VI. Measured values of nonlinear absorption coefficient and nonlinear refractive index of ZnO–TiO_2–SiO_2 nanocomposites at an intensity of 300 MW/cm^2 for an irradiation wavelength of 532 nm.

ZnO–TiO_2–SiO_2 nanocomposites	β cm/GW	n_2 10^{-17} m^2/W
SiO_2	1.7	−0.9
TiO_2–SiO_2	27.7	−3.1
1ZnO–TiO_2–SiO_2	51.8	−3.8
2ZnO–TiO_2–SiO_2	86.4	−5.0
3ZnO–TiO_2–SiO_2	110.6	−6.7
5ZnO–TiO_2–SiO_2	155.5	−9.5

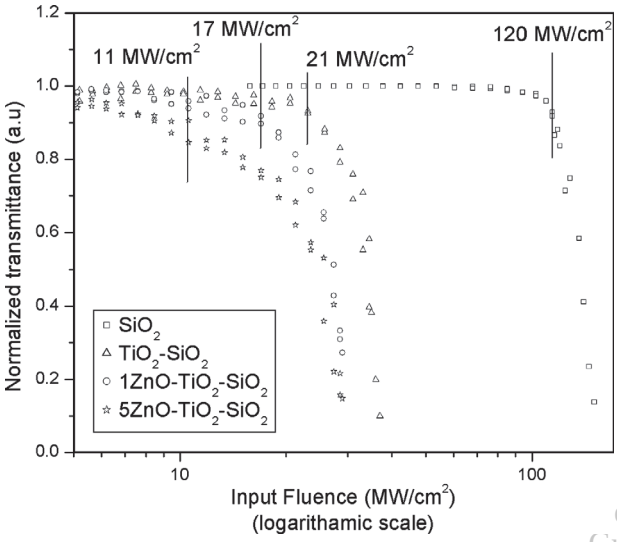

Fig. 37. Optical limiting response of ZnO–TiO_2–SiO_2 nanocomposites.

in absorption with the ZnO content and as the volume fraction of ZnO increases, the excitonic peak exhibits its signature.[39] It is seen that the absorption edge corresponding to the nanocomposites gets red shifted and the exciton oscillator strength increases as a function of the ZnO content consistent with published reports.[74]

3.6.2. Nonlinear Optical Characterization

Figure 35 shows the nonlinear absorption of ZnO–TiO_2–SiO_2 nanocomposites at a typical fluence of 300 MW/cm^2. The nonlinear absorption coefficient increases substantially in the nanocomposites, as compared to pure SiO_2 colloids. The large values of the third-order nonlinearity can be attributed to the enhancement of exciton oscillator strength.[12] We propose that this nonlinearity is caused by two photon absorption followed by weak free carrier absorption and nonlinear scattering occurring in the nanocomposites.

Figure 36 gives the closed aperture z-scan traces of ZnO–TiO_2–SiO_2 nanocomposites at a fluence of 300 MW/cm^2. The closed-aperture curve exhibits a peak–valley shape, indicating a negative value for the nonlinear refractive index n_2. It is observed that the peak–valley of closed-aperture z-scan satisfied the condition $\Delta z \sim 1.7\ z_0$, thus confirming the presence of pure electronic third order nonlinearity.[54] We suggest that the possible physical origin of the nonlinear refraction of ZnO–TiO_2–SiO_2 nanocomposites is mainly a due to two photon absorption process and partially due to nonlinear scattering and weak thermal effects in the nanosecond time domain. We have not observed any sign reversal of the nonlinear refractive index either in the intensity ranges (150–400 MW/cm^2) studied using the second harmonics of a Q-switched Nd:YAG laser or within the wavelength range 450–650 nm studied using a tunable laser (Quanta Ray MOPO, 5 ns, 10 Hz).

The obtained values of nonlinear optical parameters of ZnO–TiO_2–SiO_2 nanocomposites are shown in

Table VII. Spectral and nonlinear optical properties of ZnO nanocomposites.

Nanocomposites	Emission mechanism	Third order optical nonlinearity
ZnO–Ag	Strong UV emission	Negative nonlinearity and induced absorption due to TPA followed by weak FCA at 532 nm
ZnO–Cu	UV and visible emission	Negative nonlinearity at 532 nm Switching from SA to RSA as the excitation wavelength changes from the surface plasmon resonance to off-resonanance wavelengths Off-resonance wavelength: TPA followed by weak FCA and interband absorption Resonance wavelength: Plasmon band bleach and optical limiting mechanisms
ZnO–CdS	Emission peaks changes from 385–520 nm in proportion to changes in E_g from 2.62–3.84 eV	Negative nonlinearity at 532 nm Switching from SA to RSA as the excitation wavelength changes from the excitonic resonance to off-resonanance wavelengths Off-resonance wavelength: TPA followed by weak FCA Resonance wavelength: Exciton bleach and optical limiting mechanisms
ZnO–TiO_2	Emission peaks changes from 340–385 nm for changes in E_g from 3.84–4.12 eV	Negative nonlinearity and induced absorption due to TPA followed by weak FCA at 532 nm
ZnO–SiO_2	Strong UV emission	Negative nonlinearity and induced absorption due to TPA followed by weak FCA and nonlinear scattering at 532 nm
ZnO–TiO_2–SiO_2	—	Negative nonlinearity and induced absorption due to TPA followed by weak FCA and nonlinear scattering at 532 nm

Table VI. The nanocomposites exhibit induced absorption at all wavelengths and good nonlinear absorption, which increases with increase in input intensity. The nonlinear refractive index increases substantially in the nanocomposites, as compared to pure SiO_2 colloids.

3.6.3. Optical Limiting

Figure 37 illustrates the influence of volume fraction of ZnO in ZnO–TiO_2–SiO_2 nanocomposites on the optical limiting response. The optical limiting threshold is found to be very low in the case of TiO_2–SiO_2 colloids (21 MW/cm^2) in comparison with that of the silica colloids (120 MW/cm^2). ZnO–TiO_2–SiO_2 nanocomposites are found to be good optical limiters compared to ZnO, TiO_2 and SiO_2 and the optical limiting threshold of 5ZnO–TiO_2–SiO_2 nanocomposites is observed to be 11 MW/cm^2. Nanocomposites have a significant effect on the limiting performance and increasing the volume fraction of ZnO reduces the limiting threshold and enhances the optical limiting performance.

REVIEW

4. CONCLUSIONS

The spectral and nonlinear optical properties of ZnO based nanocomposites prepared by colloidal chemical synthesis are investigated and are summarized in Table VII. The large values of the third-order nonlinearity in the composites can be attributed to the enhancement of exciton oscillator strength. ZnO nanocomposites have high UV absorption and low nonlinear optical limiting threshold than nano ZnO. ZnO–CdS and ZnO–TiO_2 nanocomposites show tunable light emission. We get a particular light emission from UV to green just by changing the composition of these nanocomposites. ZnO nanocomposites are highly nonlinear and transparent too and so it can be used to make Googles. Thus ZnO based nanocomposites are potential materials for the light emission and for the development of nonlinear optical devices with a relatively small limiting threshold.

References and Notes

1. U. Kreibig and M. Vollmer, Optical Properties of Metal Clusters, Springer, Berlin **(1995)**.
2. B. Kraeutler and A. J. Bard, *JACS* 100, 4317 **(1978)**.
3. T. Sekino, T. Nakajima, S. Ueda, and K. Niihara, *J. Am. Ceram. Soc.* 80, 1139 **(1997)**.
4. A. E. Hichou, A. Bougrine, J. L. Bubendorff, J. Ebothe, M. Addou, and M. Troyon, *Semicond. Sci. Technol.* 17, 607 **(2002)**.
5. X. H. Wang, J. L. Shi, S. G. Dai, and Y. Yang, *Thin Solid Films* 429, 102 **(2003)**.
6. L. Irimpan, A. Deepthy, Bindu Krishnan, V. P. N. Nampoori, and P. Radhakrishnan, *J. Appl. Phys.* 102, 063524 **(2007)**.
7. D. M. Bagnall, Y. F. Chen, Z. Zhu, T. Yao, S. Koyama, M. Y. Shen, and T. Goto, *Appl. Phys. Lett.* 70, 2230 **(1997)**.
8. U. Ozgur, Y. I. Alivov, C. Liu, A. Teke, M. A. Reshchikov, S. Dogan, V. Avrutin, S. J. Cho, and H. Morkoc, *J. Appl. Phys.* 98, 041301 **(2005)**.
9. A. Tsukazaki, A. Ohtomo, T. Onuma, M. Ohtani, T. Makino, M. Sumiya, K. Ohtani, S. F. Chichibu, S. Fuke, Y. Segawa, H. Ohno, H. Koinuma, and M. Kawasaki, *Nat. Mater.* 4, 42 **(2005)**.
10. Y. Sun, J. E. Riggs, K. B. Henbest, and R. B. Martin, *J. Nonlinear Opt. Physics and Materials* 9, 481 **(2000)**.
11. K. Uchida, S. Kaneko, S. Omi, C. Hata, H. Tanji, Y. Asahara, A. J. Ikushima, T. Tokizaki, and A. Nakamura, *J. Opt. Soc. Am. B, Opt. Phys.* 11, 1236 **(1994)**.
12. A. P. Alivisatos, *J. Phys. Chem.* 100, 13226 **(1996)**.
13. L. E. Brus, *J. Chem. Phys.* 79, 5566 **(1983)**.
14. M. V. Rama Krishna and R. A. Friesner, *Phys. Rev. Lett.* 67, 629 **(1991)**.
15. N. Suzuki, Y. Tomita, and T. Kojima, *Appl. Phys. Lett.* 81, 4121 **(2002)**.
16. S. X. Wang, L. D. Zhang, H. Su, Z. P. Zhang, G. H. Li, G. W. Meng, J. Zhang, Y. W. Wang, J. C. Fan, and T. Gao, *Phys. Lett. A* 281, 59 **(2001)**.
17. P. Yang, C. F. Song, M. K. Lu, X. Yin, G. J. Zhou, D. Xu, and D. R. Yuan, *Chem. Phys. Lett.* 345, 429 **(2001)**.
18. M. Y. Han, W. Huang, C. H. Chew, L. M. Gan, X. J. Zhang, and W. Ji, *J. Phys. Chem. B* 102, 1884 **(1998)**.
19. A. Nakamura, Y. L. Lee, T. Kataoka, and T. Tokizaki, *J. Lumin.* 60–61, 376 **(1994)**.
20. L. Irimpan, A. Deepthy, Bindu Krishnan, V. P. N. Nampoori, and P. Radhakrishnan, *Appl. Phys. B: Lasers and Optics* 90, 547 **(2008)**.
21. E. S. P. Leong and S. F. Yu, *Adv. Mater.* 18, 1685 **(2006)**.
22. Chennupati Jagadish and Stephen J. Pearton, Zinc Oxide: Bulk, Thin Films and Nanostructures: Processing, Properties and Applications, Elsevier, France **(2006)**.
23. J. Piprek, Semiconductor Optoelectronic Devices: Introduction to Physics and Simulation, Academic press, Elsevier-USA **(2003)**.
24. J. A. Van Vechten and T. K. Bergstresser, *Phys. Rev. B* 1, 3351 **(1970)**.
25. W. W. Chow and S. W. Koch, Semiconductor Laser Fundamentals, Springer, Berlin **(1999)**.
26. R. Zimmermann, Many Particle Theory of Highly Excited Semiconductors, Teubner Verlagsgesellschaft, Leipzig **(1998)**.
27. V. Palankavski, G. K. Grujin, and S. Selberherr, *Mater. Sci. Eng. B* 66, 46 **(1999)**.
28. D. B. M. Kaassen, J. W. Slotboom, and B. C. de Graff, *Solid. Stat. Electron.* 35, 125 **(1992)**.
29. L. Irimpan, Bindu Krishnan, A. Deepthy, V. P. N. Nampoori, and P. Radhakrishnan, *J. Phys. D: Appl. Phys.* 40, 5670 **(2007)**.
30. L. Irimpan, V. P. N. Nampoori, and P. Radhakrishnan, *Chem. Phys. Lett.* 455, 265 **(2008)**.
31. L. Irimpan, V. P. N. Nampoori, and P. Radhakrishnan, *J. Mater. Res.* 23, 2836 **(2008)**.
32. L. Irimpan, V. P. N. Nampoori, and P. Radhakrishnan, *J. Appl. Phys.* 103, 094914 **(2008)**.
33. L. Irimpan, Bindu Krishnan, V. P. N. Nampoori, and P. Radhakrishnan, *J. Colloid Interface Sci.* 324, 99 **(2008)**.
34. L. Irimpan, V. J. Dann, Bindu Krishnan, A. Deepthy, V. P. N. Nampoori, and P. Radhakrishnan, *Laser Physics* 18, 882 **(2008)**.
35. L. Irimpan, Bindu Krishnan, V. P. N. Nampoori, and P. Radhakrishnan, *Appl. Opt.* 47, 4345 **(2008)**.
36. M. S. Bahae, A. A. Said, T. H. Wei, D. J. Hagan, and E. W. Van Stryland, *IEEE J. Quantum Electron.* 14, 760 **(1990)**.
37. L. Irimpan, D. Ambika, V. Kumar, V. P. N. Nampoori, and P. Radhakrishnan, *J. Appl. Phys.* 104, 033118 **(2008)**.
38. L. Irimpan, Bindu Krishnan, V. P. N. Nampoori, and P. Radhakrishnan, *Opt. Mater.* 31, 361 **(2008)**.
39. D. L. Moreno, E. D. Rosa-Cruz, F. J. Cuevas, L. E. Regalado, P. Salas, R. Rodriguez, and V. M. Castano, *Opt. Mat.* 19, 275 **(2002)**.

40. S. Patole, M. Islam, R. C. Aiver, and Shailaja Mahamuni, *J. Mater. Sci.* 41, 5602 **(2006)**.
41. T. Linnert, P. Mulvaney, and A. Henglein, *J. Phys. Chem.* 97, 679 **(1993)**.
42. A. L. Stroyuk, V. V. Shvalagin, and S. Ya Kuchmii, *Theor. Exp. Chem.* 40, 98 **(2004)**.
43. L. Duan, B. Lin, W. Zhang, S. Zhong, and Z. Fua, *Appl. Phys. Lett.* 88, 232110 **(2006)**.
44. L. D. Zhang and J. M. Mou, Nanomaterials and Nanostructures, Scientific, Beijing, China **(2001)**.
45. R. Reisfeld, M. Eyal, and D. Brusilovsky, *Chem. Phys. Lett.* 153, 210 **(1988)**.
46. B. Karthikeyan, M. Anija, and R. Philip, *Appl. Phys. Lett.* 88, 053104 **(2006)**.
47. X. J. Zhang, W. Ji, and S. H. Tang, *J. Opt. Soc. Am. B* 14, 1951 **(1997)**.
48. P. V. Kamat, M. Flumiani, and G. V. Hartland, *J. Phys. Chem. B* 102, 3123 **(1998)**.
49. T. S. Ahmadi, S. L. Logunov, and M. A. El Sayed, *J. Phys. Chem.* 100, 8053 **(1996)**.
50. R. Philip, G. Ravindra Kumar, N. Sandhyarani, and T. Pradeep, *Phys. Rev. B, Condens. Matter.* 62, 13160 **(2000)**.
51. S. Qu, Y. Song, H. Liu, Y. Wang, Y. Gao, S. Liu, X. Zhang, Y. Li, and D. Zhu, *Opt. Commun.* 20, 3283 **(2002)**.
52. M. S. Bahae, A. A. Said, and E. W. van Stryland, *Opt. Lett.* 14, 955 **(1989)**.
53. Y. Hamanaka, A. Nakamura, S. Omi, N. Del Fatti, F. Vallee, and C. Flytzanis, *Appl. Phys. Lett.* 75, 1712 **(1999)**.
54. D. H. Osborne, Jr., R. F. Haglund, Jr., F. Gonella, and F. Garrido, *Appl. Phys. B, Lasers and Opt.* 66, 517 **(1998)**.
55. W. Gang, Z. Yu, C. Yiping, D. Muyun, and L. Mi, *Opt. Commun.* 249, 311 **(2005)**.
56. P. Prem Kiran, G. De, and D. Narayana Rao, *IEE Proc.-Circuits Devices Syst.* 150, 559 **(2003)**.
57. G. Yang, D. Guan, W. Wang, W. Wu, and Z. Chen, *Opt. Mater.* 25, 439 **(2004)**.
58. S. Shi, W. Ji, and S. H. Tang, *J. Am. Chem Soc.* 116, 3615 **(1994)**.
59. W. Jia, E. P. Douglas, F. Guo, and W. Suna, *Appl. Phys. Lett.* 85, 6326 **(2004)**.
60. L. Irimpan, Bindu Krishnan, A. Deepthy, V. P. N. Nampoori, and P. Radhakrishnan, *J. Appl. Phys.* 103, 033105 **(2008)**.
61. A. A. Khosravi, M. Kundu, L. Jatwa, S. K. Deshpande, U. A. Bhagwat, M. Sastry, and S. K. Kulkarni, *Appl. Phys. Lett.* 67, 18 **(1995)**.
62. H. S. Kang, J. S. Kang, S. S. Pang, E. S. Shim, and S. Y. Lee, *Mater. Sci. Eng. B* 102, 313 **(2003)**.
63. A. Suzuki and S. Shionoya, *J. Phys. Soc. Jpn.* 31, 1455 **(1971)**.
64. P. Peka and H. J. Schulz, *Physica B* 193, 57 **(1994)**.
65. B. Karthikeyan, J. Thomas, and R. Philip, *Chem. Phys. Lett.* 414, 346 **(2005)**.
66. Y. Gao, X. Zhang, Y. Li, H. Liu, Y. Wang, Q. Chang, W. Jiao, and Y. Song, *Opt. Commun.* 251, 429 **(2005)**.
67. S. K. Panda, S. Chakrabarti, B. Satpati, P. V. Satyam, and S. Chaudhuri, *J. Phys. D: Appl. Phys.* 37, 628 **(2004)**.
68. S. Shionoya and W. M. Yen, Phosphor Handbook, CRC press, New York **(1999)**.
69. J. He, W. Ji, G. H. Ma, S. H. Tang, H. I. Elim, W. X. Sun, Z. H. Zhang, and W. S. Chin, *J. Appl. Phys.* 95, 11 **(2004)**.
70. R. A. Ganeev, A. I. Ryasnyansky, R. I. Tugushev, and T. Usmanov, *J. Opt. A: Pure Appl. Opt.* 5, 409 **(2003)**.
71. N. Venkatram, R. Sai Santosh Kumar, and D. Narayana Rao, *J. Appl. Phys.* 100, 074309 **(2006)**.
72. R. F. de Farias, *J. Colloid Interface Sci.* 239, 584 **(2001)**.
73. A. Penzkofer and W. Falkenstein, *Opt. Commun.* 17, 1 **(1976)**.
74. H. I. Elim, W. Ji, A. H. Yuwono, J. M. Xue, and J. Wang, *Appl. Phys. Lett.* 82, 2691 **(2003)**.
75. Y. Watanabe, M. Ohnishi, and T. Tsuchiya, *Appl. Phys. Lett.* 66, 3431 **(1995)**.
76. A. Kurian, K. P. Unnikrishnan, Pramod Gopinath, V. P. N. Nampoori, and C. P. G. Vallabhan, *J. Nonlinear Opt. Phys. & Mats.* 10, 415 **(2001)**.
77. Sun, J. P. Longtin, and P. M. Norris, *J. Non-Cryst. Solids* 281, 39 **(2001)**.
78. T. Olivier, F. Billard, and H. Akhouayri, *Opt. Express* 12, 1377 **(2004)**.
79. J. T. Seo, S. M. Ma, Q. Yang, L. Creekmore, H. Brown, R. Battle, K. Lee, A. Jackson, T. Skyles, B. Tabibi, K. P. Yoo, S. Y. Kim, S. S. Jung, and M. Namkung, *Journal of the Korean Physical Society* 48, 1395 **(2006)**.

Received: 7 June 2009. Accepted: 28 January 2010.